

**POLITECNICO DI TORINO**

**Corso di Laurea Magistrale  
in Engineering Mechanics**

**Numerical Study of Thermal Management and  
Validating Experiments of a Data Center**



**Relatori**

Prof. Alfonso Capozzoli

**Co-Relatori**

Prof. Marco Simonetti

**Candidato**

Abtin Hesami

Aprile 2019

# Table of Contents

Notation.....	3
Summery.....	5
Chapter 1 Data center.....	6
1.1. General description of the data center.....	6
1.2. Importance of CFD.....	10
1.3. Data center thermal management.....	11
1.4. Thermal metrics.....	13
Chapter 2 Data center model.....	18
2.1. Physical model.....	18
2.2. CFD model.....	22
2.3. Rack modeling.....	23
2.4. Perforated tile modeling.....	25
2.5. CRAH modeling.....	26
2.6. Buoyancy and radiation effects.....	27
2.7. Mesh generation and grid independent.....	28
2.8. Boundary conditions.....	31
2.9. Grid study and validation.....	32
Chapter 3 Energy efficiency of data center.....	41
3.1. Thermal metrices analysis.....	41
3.2. Supply temperature optimizations.....	49
3.3. Rack cooling indices.....	51
3.4. Return temperature index.....	53
3.5. Supply and return heat indices.....	54
Chapter 4 Thermal metrices analyzing in different scenarios.....	55

4.1. Effect of adding partitions on thermal metrics .....	56
4.1.1. Roof containment .....	56
4.1.2. Partial closing of the plenum .....	57
4.1.3. Vertical partition on top of the racks.....	58
4.2. Effect of power density on thermal metrics.....	63
Conclusion .....	70
References.....	72

## Notations

T Temperature, ( $^{\circ}\text{C}, \text{K}$ )

$A_r$  Archimedes Number

$\beta$  Volumetric thermal expansion coefficient, ( $1/\text{K}$ )

g Gravitational acceleration ( $\text{m}/\text{s}^2$ )

L Length scale, (m)

P Power, (kW)

p Pressure (Pa)

U Average velocity ( $\text{m}/\text{s}$ )

$\rho$  Density ( $\text{kg}/\text{m}^3$ )

$\sigma$  Tile porosity

$\dot{m}$  Mass flow rate ( $\text{kg}/\text{s}$ )

$\dot{V}$  Volumetric flow rate ( $\text{m}^3/\text{s}$ )

Q Total heat dissipation rate from the racks in the data center (W)

$Q_{total}$  Total facility power consumption rate of data center (W)

$\delta Q$  Enthalpy flow rate rise of the cold air before entering the racks (W)

$A_{tile}$  Physical area of tile, ( $\text{m}^2$ )

$A_{opening}$  Area of computational opening, ( $\text{m}^2$ )

F Body force per unit volume, ( $\text{N}/\text{m}^3$ )

$T_x$  Mean temperature at each rack intake ( $^{\circ}\text{C}$ )

$\Delta T_{equip}$  Temperature increase across IT equipment ( $^{\circ}\text{C}$ )

$\Delta T_{inlet}$  Temperature difference between CRAC supply air and rack inlet ( $^{\circ}\text{C}$ )

$\Delta T_{rack}$  Temperature rise through the server racks ( $^{\circ}\text{C}$ )

$T_{ref}$  Reference temperature ( $^{\circ}\text{C}$ )

$\forall$  Volume ( $\text{m}^3$ )

## **DC data center**

ADS Air distribution system

UFAD Underfloor Air distribution system

RH Relative humidity

RHI Return heat index

RCI Return cooling index

RTI Return temperature index

SHI Supply heat index

IT Information technology

CFD Computational Fluid Dynamics

CRAC Computer Room Air Condition

RANS Reynolds-Averaged Navier-Stokes

## **Subscribe**

in Inlet

out Outlet

Tref CRAC supply temperature

max-rec Maximum recommended

max-all Maximum allowable

min-rec Minimum recommended

min-all Minimum allowable

## Summary

The worldwide demand for storage of data continues rapidly so the number and size of the data center are increasing constantly. Significant power consumption is dedicated in the U.S in 2006 nearly 1.5% percent of overall electricity consumption in the U.S. and as a matter of fact, up to half of this power is spending in cooling of facilities (computer room air condition (CRAC) or computer room air handler (CRAH) in a data center. As energy consumption is huge the energy efficiency is an important issue to consider in the data center. Computation fluid dynamics (CFD) can be very useful in order to provide detail information about the airflow behavior in the existing data center and simulating a data center before it is built. How to simulation needed to carry Out with quality and trust. In this study and existed data center located in Research Lab at Syracuse University which was simulated by ASNSY Fluent and validated by experimental data with the same boundary condition is used as a model. The academic code ANSYS Icepak 15.0 is used for simulation. Two different grid study and Realizable k-epsilon turbulent and normal k-epsilon turbulence air flow model is applied to compare the temperature profile against the experimental data, in the next chapter I analyses the energy efficiency of the model by typically the non-dimensional parameters that proposed. And as the inlet temperature of the lower server chassis were relatively lower than the recommended values proposed by ASHRAE, I tried to find the maximum allowable temperature according to the ASHRAE limitation metric parameter. simultaneously I figured out the influence of using different temperature supply on thermal metrics so different logical supply temperature (13°C, 15°C, 16°C,17°C and 18°C are chosen and studied. In the next chapter, I applied the adiabatic surface portions as a roof containment (horizontally ) to cover the surface between the top of the rack and front wall, vertical portion on the top of the rack and closing a portion of the under-floor plenum. To understand their effect on thermal matrices, and in the next chapter different I study the influence of increasing power on thermal matrices, to figuring out this effect default rack power compared by increasing the current power to 10%,20%, and 40 %.

# Chapter 1

## Data center

### 1.1 General description of the data center

A Data center is a structure include of networks, IT servers and data storage of organization and business enterprise which provides services such as storage, process and disseminate a large amount of data. To ensure that these computer servers working reliably, they must be adequately and continuously cooled. Over temperature at the intake of racks caused not only more power consumption but also a failure of a server and losing the data of an organization. While over the cooling outcome is consuming useless energy for cooling of the facilities. Considering a huge power consumption of data center, the importance a proper design is more and more every day. Air recirculation and air bypass around which causes non-uniform temperature air distribution at the inlet of the server's racks are the unpleasant phenomena for reliable operation and energy consumption of data centers. By advancement of science and technology management and the process of a huge amount of data storages, causes the exponential growth the data center in number and size over the world. The major issue in DC is that they are consuming huge energy. Some huge centers electricity bills arrive up to millions of dollars [1]. In 2013 Natural Defense Counsel report, announced that the data centers in United State consumed 91 billion of energy, and claims that this energy consumption will peak to 140million kW of energy in 2020. [2] predict that data centers in the world will consume 8% of total electrical energy. Obviously, it is extremely important to manage this high-power consumption and improve system performance. Patterson [3] divided into 3 main sources of energy consumption in a data center:

- Loads: servers racks which include Chipset, Hard Disk drives (HDDs) processing units (CPUs), Memories.
- Power delivery: Power supply unit (PSU), Power Delivery Unit (PDU), Unterminated power supply (UPS)
- Cooling: Chillers, Computer Room Air condition (CRAC), Computer Room Air Handler (CRAH), fans, server fan and, pumps

It's interesting that the energy consumption for the cooling system in DC is in range of 24%-60% of total energy that consumed in data center [4]. This high range of consumption is because of different types of IT equipment, air distribution system and the configuration of the server room. Increasing the efficiency of each member of this source would be important, but there is another source of inefficiency should be considered which is Air distribution system (ADS). It means the way that the cooled air brought to the inlet of the racks and returned from exiting the rack to the air conditioning unit, which could influence on cooling performance. On the other word improving the airflow is an idea to decrease the energy cost of the cooling system in a data center.in **Fig.1** a typical data center with under-floor air distribution and false ceiling consist of racks CRAC is represented. The cold air from under from the bottom of CRAC and throw the perforated tiles entering cold aisle and the cold air sucked by rack intake and cool the server racks and the warm air from the back of the server exiting and turn back through the ceiling return the air conditioning unit, and this cycle working continuously. In the current study, our control volume is inside the data center facility.

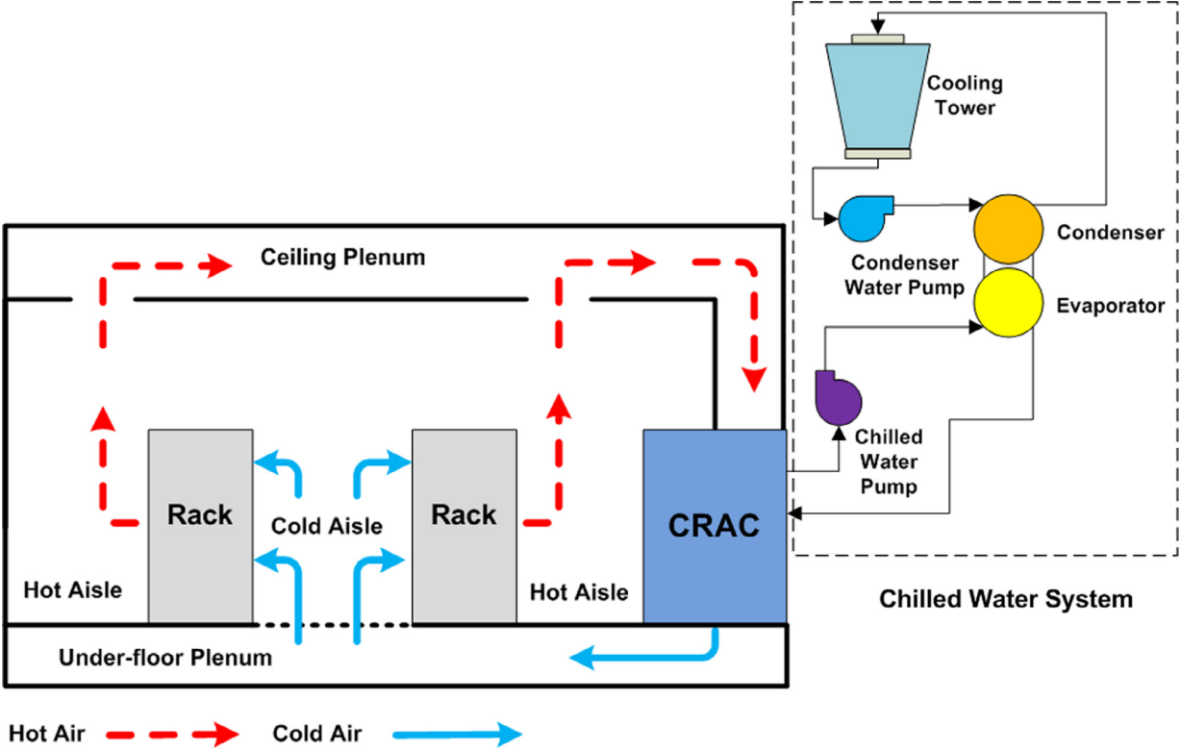


**Fig 1.** A typical data center consists of Racks CRAC(H) cold aisle and hot aisles.

Generally, each cooling distribution system has a supply and return section. The supply section energized the cold air from the air condition unit to the room with fan and return system takes the hot air return to the back of the air conditioning unit. There are air different airflow distribution configurations were studied by [6] and other authors fully duct configuration is not very common because of the space limitation and maintenance problems, nearly all the authors agreed on best configuration by considering security, installation, maintenance and efficiency point of view is under-floor air distribution system (UFAD) may combining by ceiling return locally duct. **Fig 2.**

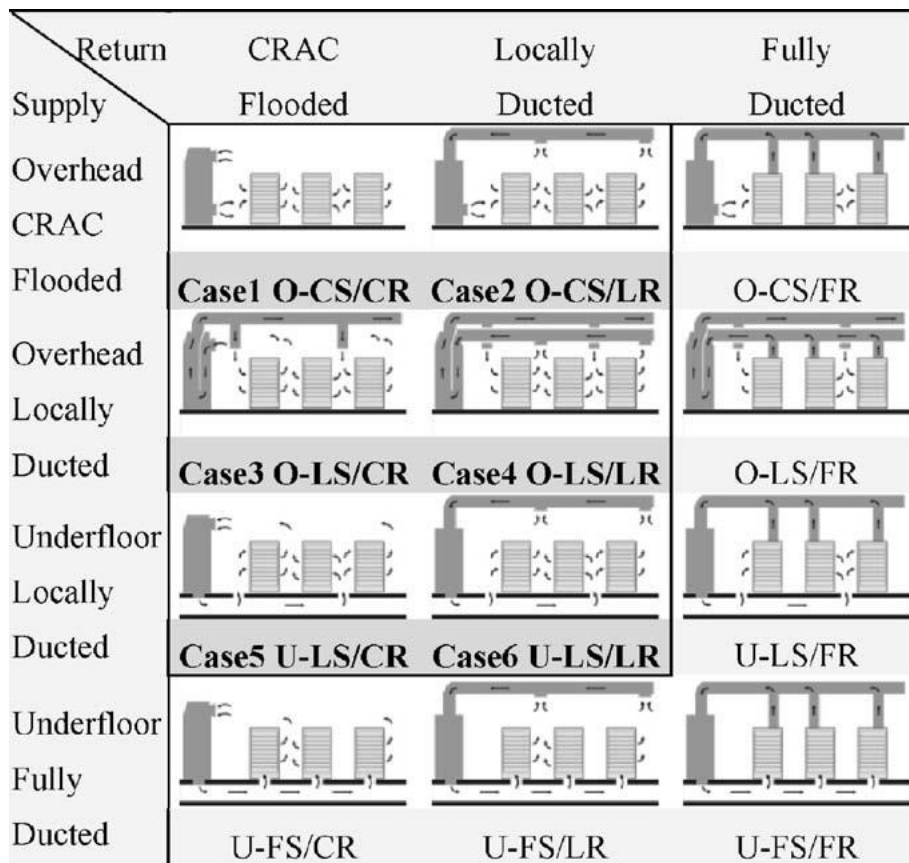


**Fig.2.** Twelve types of air distribution systems.[6]

Majority of the server which is mounted racks are designed to sucking air from the front part and exhaust it at the rear of the unit. Therefore, in order to have a better air reciliation, the intake air region and exhaust air of the region of IT compartments are separate to different areas. The best-case scenario is to configure the compartment in intermittent cold and hot. Cold aisles include the floor tiles or diffusers that cold air from the CRAH supply passing over the underfloor plenum and exiting from the perforated tiles in the cold aisle, generally two racks in front of each other sucking the cold air. Or in the other word racks are arranged in order to all servers' intake face cold aisles. If all rows equipped in the same way with front facing, equipment malfunction is indispensable. The reason is that due to the large data center and many IT serves, a proper solution which is implemented to place air intake and outtake of the servers at separate locations for effective server cooling. Mission critical facilities, technologies, and electronic equipment provide thermal guide lines for data processing environment Table 1. This table demonstrates the best configuration distance of hot and cold aisle, and the size of the tiles by considering the safety parameters, easy installing and repairing. As it is showing in **table 1**[7] the standard tile size in U.S standard is 610mm and the cold- aisle size is 1220mm and hot aisle 914mm and the minimum distance to the wall must be equal to 1220mm. The standard rack length is 997mm the pitching aisle which is the distance between the center of 2 parallel cold aisles is equal to 7 tiles or 427mm.

	Tile size	Aisle pitch	Cold-aisle size	Hot-aisle size
U.S.	2 ft (610 mm)	14 ft (4267 mm)	4 ft (1220 mm)	3 ft (914 mm)
Global	600 mm (23.6 in)	4200 mm (13.78 ft)	1200 mm (3.94 ft)	914 mm (3 ft)

Seven-tile aisle pitch, equipment aligned on cold aisle|

**Table 1** Aisle pitch allocation and rack arrangement with separation [7]

## 1.2 Importance of CFD

The computational fluid dynamic is an application of fluid mechanics that uses numerical analysis and modeling the structure and solving the problem of fluid flows. Computers provide this calculation with a define boundary condition and simulation models. CFD can be utilized in a wide range of engineering problems and researches. The importance and application of CFD simulation are increasing over time, as it is needed to have intelligence design and upgrade the previous models. A remarkable issue is that the CFD code which we are applying in a specific design is appropriate to our simulation. Using software, right turbulent model, the proper boundary condition is a prerequisite subject for the simulation of a model. CFD simulation is needed to be validated against the experimental data to be sure that can trust the simulation model. Of course, the prediction of simulation is not precise, and CFD software is updating to get more accurate prediction respect to experimental data. Most recent studies of CFD simulation focused on enhancing the design of the data center model to improve its efficiency. ANSYS Icepak uses Fluent computational fluid dynamic solver engine to calculate fluid flow and thermal parameters which geometry and boundary condition, and mesh generation and CFD setting parameters are design and set in Icepak. The basic equation for all the flows ANSYS Fluent solving the equation of conservation law for mass, momentum, and energy. additional transport equations are solved when the flow is turbulent. In turbulent flows, the variables are decomposing in into mean value and the deviation value, while the mean value is the important part. By the decomposing, the variable in Naiver-stocks equation and in certain time average, governing equation of steady mean flow can be obtained .[10].Basic equation for mass conservation and momentum conservation are:

$$\frac{\partial \rho}{\partial t} + \nabla \cdot (\rho \vec{v}) = 0 \quad (1)$$

$$\frac{\partial}{\partial t} (\rho \vec{v}) + \nabla \cdot (\rho \vec{v} \vec{v}) = -\nabla p + \nabla \cdot (\bar{\tau}) + \rho \vec{g} + \vec{F} \quad (2)$$

where  $p$  is the static pressure,  $\bar{\tau}$  is the stress tensor , and  $\rho \vec{g}$  and  $\vec{F}$  are the gravitational body force and external body forces (e.g., that arise from interaction with the dispersed phase), respectively.  $\vec{F}$  also contains other model-dependent source terms such as porous-media and user-defined sources [9]

### 1.3 Data Centre thermal management

Non-uniform air distribution at the inlet of the server's rack is the major problem in data centers, unfortunately, the main role of the data center air distribution system is avoiding overheating of IT equipment. In a typical under-floor air distribution system, cold air from CRAH(C) passes through the perforated tiles and is guided to the chassis of the server to reduce the temperature of IT servers, some of the cooled air provided by CRAH(C) may not be taken by the racks (by-pass air) **Fig.[3]**, and directly returns to the CRAH(C) which is not taken seriously in data centers as it is not dangerous but it's important to reduce it in order to improve the efficacy of data center. As a matter of fact, By-pass air influences the cold temperature produced by CRAH(C) and the inlet temperature of the IT servers. By-pass air which is not taken by the servers and crosses over, so the racks remain warmer and consequently let the re-circulation air enter the servers, another unpredicted rare phenomenon is negative flow which occurs in high-velocity under-floor because of the venturi effect and the air in room goes back to the tiles and increases the supply temperature [10]. The target of air management is keeping the air-bypass of cold air and recirculation of hot air to the minimum in order to provide uniform and appropriate temperature of the air at the entrance of servers, and the result will be better thermal management and efficiency. Improving air management is the result of efficiently maintaining the air flow. Flexibility is another issue that may cause some difficulties to enhance the thermal performance of a built data center [11], in this case by providing additional objects such as ceiling contaminating roof may improve the efficacy vice versa by increasing the server power load there would be a possibility to manage the extra heat generated by racks in current main facilities in the server room. It is expected that CRAH(C) supply the cold-air for the server racks and after heat removing the IT equipment's turns back to the CRAH(C), but in reality unpleasant factors such as re-circulation and by-pass and also short-circuiting decrease the cooling efficiency and cause increasing of local temperature [10], By measuring the temperature distribution at front and back side of the racks[10] and there is a chance to improve the thermal properties of server room. Supply cooled air provided by the CRAH(C) after crossing the under-floor distribution and air diffuser can provide a constant temperature at the lower part of the servers but due to air re-circulation of hot air which is generated by the racks which has lower density moves to the upper part of the servers and consequently increases at the

inlet temperature of serves occurs[10]and the result is more energy losses and power more consumption for cooling system and server malfunction.

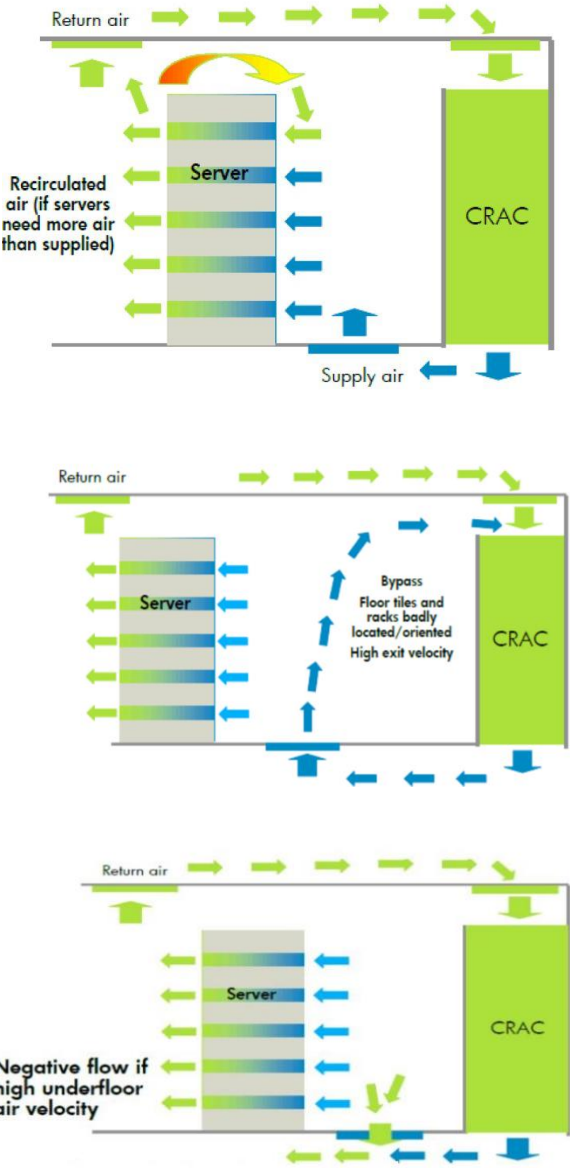


**Fig 3.** out-of-control airflow in the server room. a) Re-circulation air flow b) by-pass airflow c) negative pressure [10]

## 1.4 Thermal metrics

The grade of thermal performance of a data center basically evaluated by the temperature at the intake of servers [12], American Society of Heating, Refrigerating and Air-Conditioning Engineers (ASHRAE) [12], publishes an energy standards and guidelines relating for data center minimum standards and minimum efficiency that required to design and construction of a data center. ASHRAE issued thermal guideline classes for IT equipment for the first in 2004[12]. and still is updating **Fig.4. Table 2.** includes [12] of four class and allowable rack inlet temperature and a recommended envelope. In A1 class of ASHRAE allow the temperature range of 15°C-32°C and in the A2 class allows the temperature range of 10°C-35°C which new equipment is designed in this range, A3 class allows the temperature range of 5°C -40°C and A4 class allows the temperature still wider range of temperature 5°C -45°C to support the new energy-saving technology like economization. The original ASHRAE recommended and allowable (A1 class) rack intake temperature was 20°C-25°C and 15°C-32°C which was very conservative consideration, Reliability is the primary issue and the costs is the secondary issue. ASHRAE TC9.9 recommended 18-27°C range for rack intake temperature for normal data centers with a relative humidity of 60%, however, the old data centers were designed in a different range of temperature. According to [ASHREA] the life-time of data centers are in the range of 15 to 20 years, so the equipment of the data center may be original from the time they have built, while some have changed.

Rack cooling index (**RCI**), is firstly introduced by Herlin [15,16]. this parameter uses to measure to understand how effectively equipment racks are cooled. This index is related to rack inlet temperature. The RCI two different indexing.

$$RCI_{HI} = \left[ 1 - \frac{\text{Total over temperture}}{\text{Maxallowable over temperture}} \right] 100\% \quad (3)$$

$$RCI_{LO} = \left[ 1 - \frac{\text{Total under temperture}}{\text{Maxallowable under temperture}} \right] 100\% \quad (4)$$

RCI<sub>Hi</sub> is the most important parameter in designing of a data center which presents the working reliability of the plant a low value for this index may not only increase the power consumption but also may cause system failure. In order to calculate the value of RCI<sub>Hi</sub>, for each rack it is needed to verify the intake temperature of each server, and the total over temperature respect to, maximum recommended temperature proposed by ASHRAE **Fig 5.**, i.e. if there is no chassis that the average temperatures over the 25°C it means value for RCI<sub>Hi</sub> 100% which is ideal, usually upper parts of the rack are victims of overheating and this phenomenon occurs mainly at the upper part of the server, and 65% of the total system impairments occur at the upper third of the rack server, resulting in considerably large economic losses from server malfunctions and breakdowns[17], RCL<sub>Lo</sub> is the second important index should be considered in designing which represent the level of overcooling in the data center this value alike RCI<sub>Hi</sub> evaluate by the ASHRAE recommendation envelope. If the average temperature of any server rack is below 17°C .this value calculated by the sum of the total under the temperature of the server chassis in each rack over the minimum recommended temperature 17°C proposed by ASHRAE by equation (4). If the intake temperature of all server racks in the data center is more than 17°C it means this index value is 100%.

Rating	RCI
Ideal	100%
Good	≥ 96%
Acceptable	91-95%
Poor	≤ 90%

**Table 4.**Rack cooling rate for RCI<sub>Hi</sub> and RCI<sub>Lo</sub> [35]

The best-case scenario for RCI matrices is maintaining the rack temperature in this range of 17°C - 25°C of temperature which is big challenge in data center, usually as the cooling off is provided by the perforated tiles from the bottom at the lower server racks are victims of over-cooling and above the third quarter of rack are suffering over-temperature.

Note that, in RCI equations, total over temperature and total lower temperature considered a rack with four chassis.

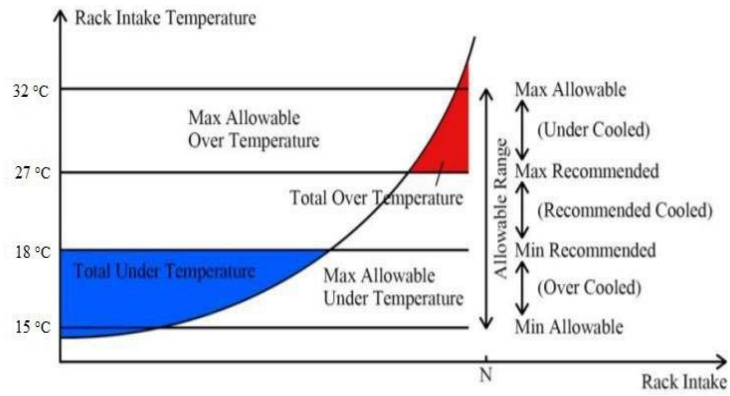


Fig 5. Definition of total over-temperature and total under temperature

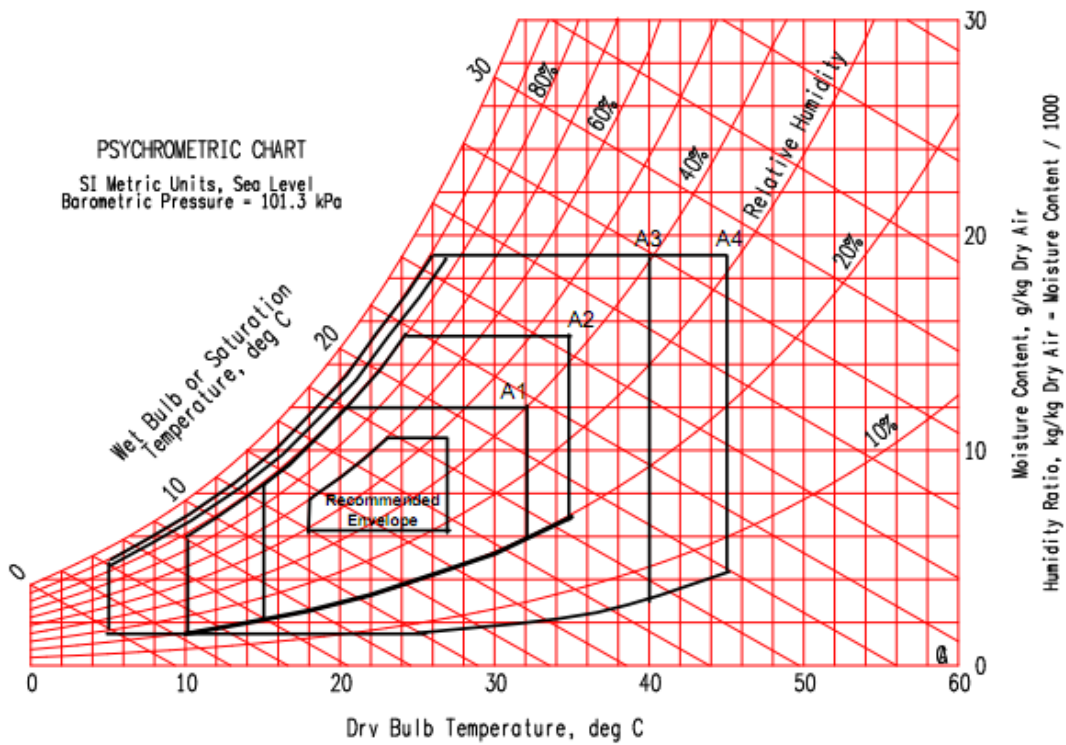


Fig 4. ASHREA environmental class for data centers [12]

Several non-dimensional parameters were used in the literature as indices of parameters in data centers. All these indices of performance based on inlet and outlet temperature of racks and the supply temperature considered as tile temperature and since temperature augmentation along air conditioning unit and perforation tiles, (CRAC(H) outlet temperature considered as reference temperature ( $T_{ref}$ ). Defining the indices of parameters help us to measure the thermal performance and efficiency of a data center. The supply heat index (SHI) dimensionless parameter [13] is defined as the ratio of the total heat gained entering the rack to total heat gained by exiting the rack and as the mass flow rate entering and exiting the rack is constant SHI can be written as:

$$SHI = \left\{ \frac{\sum_j \sum_i ((T_{in}^r)_{i,j} - T_{ref})}{\sum_j \sum_i ((T_{out}^r)_{i,j} - T_{ref})} \right\} \quad (5)$$

$$SHI = \left( \frac{\delta Q}{Q + \delta Q} \right) = \frac{\text{Enthalpy rise due to the infiltration in cold aisle}}{\text{Total enthalpy rise at rack exhaust}} \quad (6)$$

$$Q = \sum_j \sum_i m_{i,j}^r C_p ((T_{out}^r)_{i,j} - (T_{in}^r)_{i,j}) \quad (7)$$

$$\delta Q = \sum_j \sum_i m_{i,j}^r C_p ((T_{in}^r)_{i,j} - T_{ref}) \quad (8)$$

Where  $T_{ref}$  is the supply temperature of CRAH(C),  $T_{in}$  represent the average intake temperature of each server rack and  $T_{out}$  is average the temperature at the outlet of each server rack  $m_{i,j}^r$  is airflow rate mass flow rate of the  $i$ th server rack in  $j$ th row of racks,  $Q$  is the total heat dissipation rate of all the racks and  $\delta Q$  indicates as the enthalpy rise rate of cold air due to the recirculation of hot air before entering the racks. High value of SHI indicates that the inlet temperature at the entrance of rack is respectively high, which is the reason of re-circulation phenomena. SHI can be indicating the thermal performance and energy efficiency of a data center. A lower value for SHI indicates better thermal management and the best value would be 0 (typically it is < 40%). The return heat index (**RHI**) which also introduced by [13] can be written as:

$$RHI = \left\{ \frac{\sum_j \sum_i M_k C_p ((T_{in}^c)_k - T_{ref})}{\sum_j \sum_i m_{i,j}^r C_p ((T_{out}^r)_{i,j} - T_{ref})} \right\} = \frac{\text{Total heat extraction by the CRA Cunits}}{\text{Total Enthalpy rise at the rack exhaust}} \quad (9)$$

$$RHI = \left( \frac{Q}{Q + \delta Q} \right) \quad (10)$$

RHI index is the complement of SHI index so (10),(11)

$$SHI + RHI = 1$$

The return temperature index (**RTI**) which is introduced by Herlin [14] is a measure the energy performance in the air management system, this evaluation is showing the level of by-pass air or air-recirculating in a data center. as it is showing in **table 3**. The best value is 100% means all the supply air is digested by the rack while the value over 100% means some hot air from back of the server racks is added to the total mass flow rate entered to the rack and the value lower than 100% means the a portion of cold air not only digest by the racks but also crossing over the racks.

$$RTI = \left[ \frac{T_{return} - T_{supply}}{\Delta T_{equipment}} \right] 100\% \quad (12)$$

Where the  $T_{return}$  is the return air temperature of (CRAC(H) and  $T_{supply}$  is supply air temperature and  $\Delta T_{equipment}$  is the difference of average intake and exhaust server temperature.

Rating	RTI
Target	100%
Recirculation	>100%
By-pass	<100%

**Table 3.** Return temperature index value

Note that RTI value for each rack can be calculated by the average temperature supply and return CRAC over the average temperature of the inlet and exit of each rack.

# Chapter 2

## Data center model

### 2.1 Physical model

The considered data center/Research lab located at Syracuse University is shown in **Fig. 6** [18] and **Fig. 7**. (3D view). The room has a raised floor with dimension 5.64m × 7.89m and height of 3.66m and the height of under-floor plenum height is 0.76m. also, there are other obstacles such as cables smoke detection sensors and stanchions supporting raised floor which are ignored in the simulations and may make a small effect in the simulation. All the airflow distribution and cable entranced sealed to have the minimum leakage. The data center has three high power rack, and each rack consist of four chassis and the location of each rack is shown in **Fig. 6**[18], marked as R1, R2 and R3.

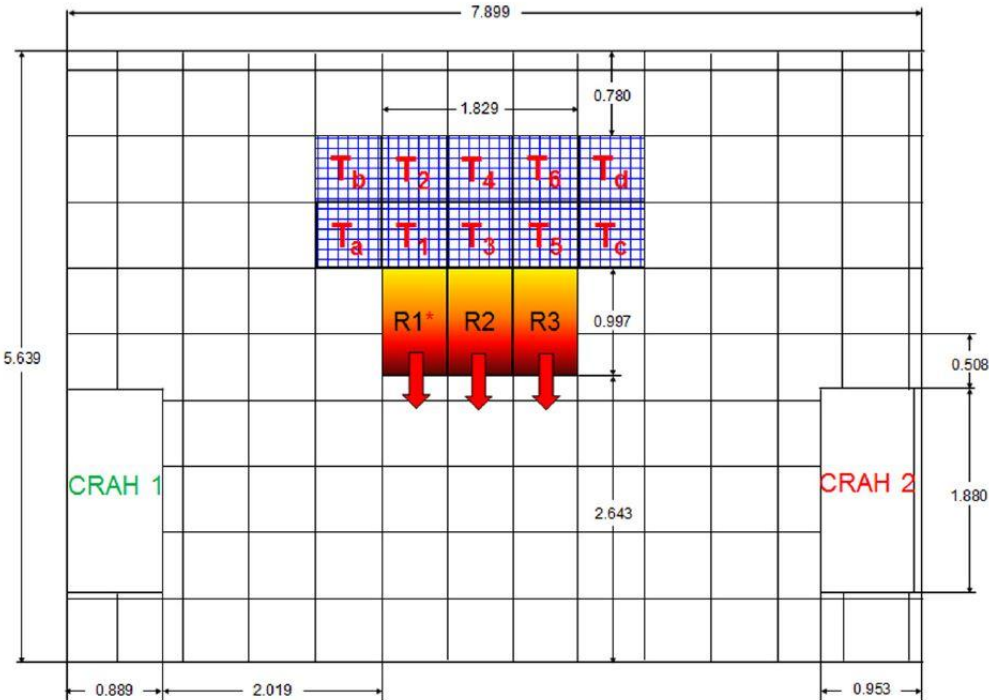


**Fig 6.** Top view of DC/RL facility

The 3D sketch of the room data center modeled in ANSYS Icepak 15.0 is presented in **Fig. 7** the control volume of the model is the cabinet that demonstrated with orange lines bounded the model, a surface in XZ plane with semitransparent gray color separated the under-floor volume and the room. there are 2 CRAHs demonstrated with gray colors. CRAH1 is located on the left side of the photo and the CRAH2 is located on the right along X-axis. Three rows of the rack with four server chassis demonstrated with blue colors and the R1 is the closest rack to the CRAH1 and the perforated tiles demonstrated in yellow color.

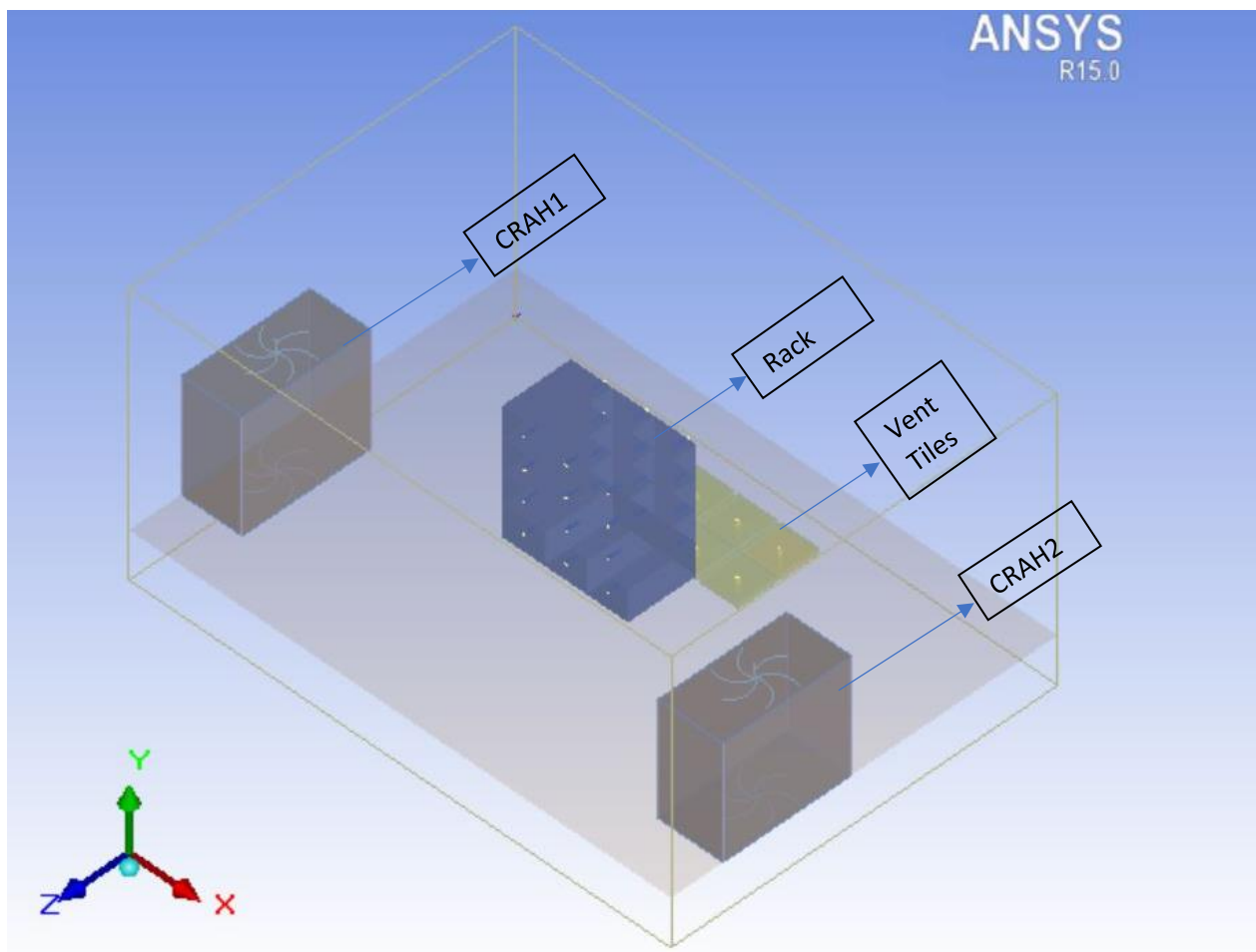


**Fig 7.** 3D sketch of DC/RL facility

Each chassis has the same geometry but two different fan type (chassis type A and B), located at the end of the rack. There are 8 heated metal plates placed at the end of each chassis, the pressure

drop in each chassis is  $\sim 300\text{Pa}$  (measured). Maximum power chassis is  $8.5\text{kW}$  ( $34\text{kW}$  per rack). type B chassis is used in R2 rack (middle rack). There are 4 fans mounted in each chassis and type A fan has a nominal flow rate of  $0.316\text{m}^3/\text{s}$  while type B fan nominal flow rate is  $0.363\text{m}^3/\text{s}$ . , 4 fans with the same catachrestic was used between heated plates and perforated screens to guarantee a nearly uniform flow at the exit of chassis. all the chassis are running with maximum flow rate and with 44% percent of maximum power. The mass flow rate is measured using a flow hood(TSI model EB721) at the exit of the racks with and without heat load, the total mass flow rate in 3-rack was  $3.965\text{m}^3/\text{s}$  .the mass flowrate of rack server was not constant and in table [21] present the detail of mass flow rate of each chassis. Considering the high power ( $\sim 35\text{kW}$ ) of a rack and high mass flow rate for each rack ( $\sim 1.4\text{m}^3/\text{s}$ ), obviously, it was needed more than one perforated tile respect to each rack for necessary cooling flow. Only three bottom rack didn't have directly influenced by re-circulating.

One CRAH (left CRAH) if **Fig.7**. is running in experimental simulation. The cooling capacity of each CRAHs is  $100\text{kW}$ . The entrance of CRAH was sealed by tapped in order to avoid any backflow. The mass flow rate measured CRAH which is equal the total mass flow rate of perforated tile is  $3.04\text{m}^3/\text{s}$ , so the ratio CRAH to the total mass flow rate of racks is 0.76%. so, it means 23% of mass flow rate dose not ingested by the rack and recirculating in the room which is common but unpleasant phenomena in data centers.in **Fig.7** the layout of perforated tile with the dimension of  $0.61\text{m}\times 0.61\text{m}$  is demonstrated. There are 6 tiles located in the front of the racks in two rows and other 4 racks placed at the sides of other racks. The average tile flow rate measured with 6 open tiles was  $0.47\text{m}^3/\text{s}$  for each tile and with normal condition (10 tiles) measured  $0.3\text{m}^3/\text{s}$  for each tile which is reasonable values, they are also verified with my study and observed the same value. The tile perforation percentage claim by the producer datasheet is 25% and in the following pages, I will focus on the detail of modeling in the simulation. According to the tile manufacture [19], the presence of damper underneath of tile perforation causes high pressure-drop and resistance at the outlet of tiles and consequently more uniform air flowrate between ten tiles. On the other word, the air velocity along above the tiles does not have significantly differences.

A straightforward measurement method is utilized to measure the temperature field in the DC/RL facility. Thermocouples (t-type with 24 gauge-wires) are connected to poles that can be

stretched out from floor to ceiling **Fig. 8** Each pole conveys up to twelve thermocouples dispersed from a height of 0.15m to a height of 3.5m over the floor (0.3m distance separation between thermocouples). These poles are utilized to quantify the vertical temperature profiles anyplace in the room by putting them at the center of each tile **Fig. 8** These temperature poles can be manually moved to play out a full scan of the temperature field in the room. Every one of the thermocouples wires are associated with a data acquisition system, which is set in a little adjoining room **Fig.8** During the data collection period, nobody was permitted to enter the DC/RL facility to keep away from any stream aggravation. More insights regarding the experimental procedures and configuration can be found in Ref. [22] Moreover, air temperature measurement all through the DC/RL facility, an array of nine thermocouples (3×3 distributed on the 0.41m 0.45m server zone) [22] utilized for estimating the temperature dispersion at the inlet and outlet of each rack. Other six thermocouples are placed at the CRAH inlet to estimate its temperature to use in CFD boundary condition also several thermocouples randomly placed along the walls.

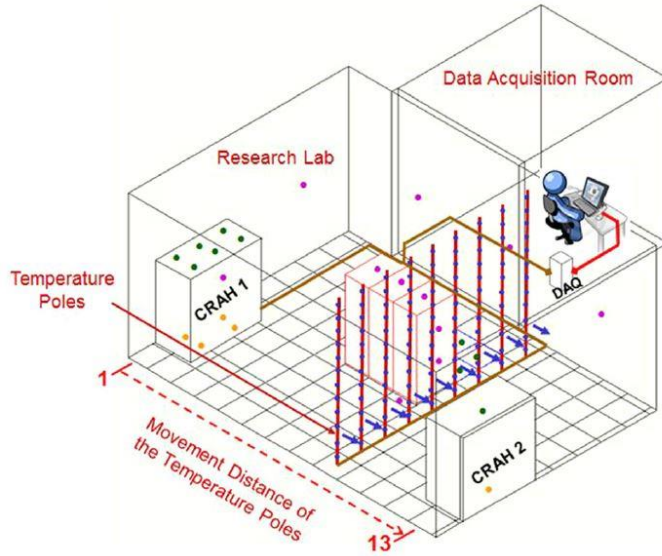


**Fig 8.** Filed measurement technique of the temperature in DC/RL facility [20]

## 2.2 CFD model

In this study, the Icepak toolbar of academic code ANSYS 15.0 is used as the software which employs FLUENT as a solver. ANSYS FLUENT software is used to a finite-volume approximation of Reynolds-averaged Navier stocks (RANS). Conservation of mass, momentum and energy are the based equation of fluid flows. each variable decomposed of the mean and fluctuating. value. In current all the CFD calculation were performed using Reynolds-averaged Navier stocks with 2<sup>nd</sup>- order precision upwind discretization scheme for convective terms, with k-epsilon realizable turbulence model and effect of wall function. In order to calculate the flow pressure and temperature distribution non-linear coupled equations were obtained. As the Mach number is  $\ll 0.3$  in data centers flow environment the air considered as an incompressible flow. The main benefit of k-epsilon Realizable turbulence model which is recently introduced respect k-epsilon model is that it has “more accurately predicts the spreading rate of both planar and round jets. It is also likely to provide superior performance for flows involving rotation, boundary layers under strong adverse pressure gradients, separation, and recirculation.” [21]. The “realizable” part means that put specific mathematical limits on the Reynolds stresses which is satisfied our model moreover consider the physics of turbulent flows. [20] used standard k-epsilon Turbulence which is the common model in CFD simulations. The results with his simulation and my work are presented in the following pages.

The simulation was run using CFD Fluent-solver. The number of iterations was set 500 and the convergence criterion of turbulent kinetic energy, turbulent dissipation rate was set 0.001 and 1e-5 for energy criteria. Each simulation converges in roughly 35 minutes with Intel core i7. The results were analyzed in CFD post which is integrated into ANSYS Ice-Pak 15 software.

## 2.3 Rack modeling

Typically, there are two different models proposed for designing racks in data centers, the first approach modeling approach is flowed network model (FNM) [23,24], in this model in addition to designing the outer part of the rack there is a possibility to generate the mesh inside the rack and study the air flow passages behavior. The main problem in this model is heavy calculation and since and it is not very recommended. Another type of rack design compact modeling in data center is called lumped model approach or black-box model [25], the main advantage of this model is computational efficacy and good adaptability not complicated calculation and analyzing in modeling. But it also suffers the information of airflow inside the racks. In this study as the target focusing on airflow behavior at the inlet and outlet of the rack, the black-box model has chosen. Each rack consists of four server chassis **Fig.9** with a measured airflow air flow rate at the exit of each rack chassis. In this model,, the mass flow rate of each chassis is specified. The power of the rack model as a black-box method in this study like [25] simulation, so we don't have any information about the internal flow path. Three racks with each four chassis are modeled as twelve boxes, the entrance, and exit of racks are open and sides, top, and bottom parts are considered as solid walls, the mass flow rate imposed at the entrance of each rack, which is measured in experiments study of [20]. In the table [5]mass flow rate of each chassis is available. The entrance section of chassis treated as outflow boundaries and the exit part treated as inflow boundaries in modeling, [26] imposed adiabatic boundary condition while for the walls, while in ANSYS Icepak 15 rack user guide [26] for rack modeling uses recirculating model for the rack simulation. The mass flow rate and heat load specified at the inlet of the rack while the inlet temperature is extrapolated from the CFD simulation. the mass flow rate considered uniform at the entrance of the rack in CFD simulation, which is not. The outlet temperature at the end of each sever in CFD simulation can be checked with a simple energy balance.

$$T_{exhaust,i} = T_{inlet,i} + \frac{Q_i}{c_p \dot{m}_i} \quad (12)$$

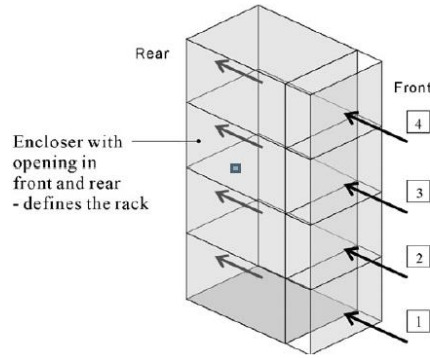


**Fig 9.**A simplified rack modeling with four chassis the photograph is [6]

The correction of momentum deficit like tile modeling is applied at the back of the racks. By adding 2 opening surfaces 0.01m to create a thin volume just behind the racks to compensate initial momentum which created because of jet initial momentum[24,27] in CFD simulations **Fig. 10.** The porosity of rack chosen the same value used in his study.

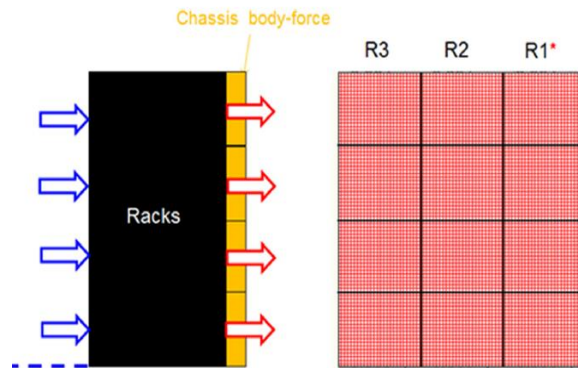


**Fig.10** side and front view of the rack model [28]

Rack 1				Rack 2				Rack 3			
R1C1	R1C2	R1C3	R1C4	R2C1	R2C2	R3C3	R4C4	R4C1	R4C2	R4C3	R4C4
0.31	0.31	0.32	0.31	0.35	0.35	0.37	0.37	0.32	0.31	0.32	0.31

**Table.5** measured chassis mass flow rate ( $m^3/s$ ) in DC/RL facility \*R1C1: the bottom chassis of rack1

## 2.4 Perforated tile modeling

A very important factor which is commonly ignored in designing of perforated tiles in the data center is the effect of momentum conversation. In the general specification of tiles production companies for data center there is parameter for the percentage of opening area, which makes some difficulties in designing tile perforation (e.g. 25%), as the surface of the tile reduces four times the velocity increases four time, and coequally produce additional initial momentum of four times, respect the fully open tile model! [28] studied the different tile configuration modeling, and Proposed a momentum surface volume in modeling tile perforation, and found that without considering the momentum source the velocity of tiles are four times more and influence the temperature of rack intake, but he did not study the effects on thermal metrics, while, consideration of momentum source deficit with perforation ratio respect to fully open ratio model(not considering the opening ratio) in inlet rack temperature does not have a notable variation. The momentum source corrects the momentum deficit of flow that passes through a fully open tile by adding a body force filed just above the tile. By assuming a fully turbulent model and flow the tile resistance (K), can be calculated by air square velocity of plenum just at the entrance of tiles, the ( $U \sim 0.81 \text{ m/s}$ ), the pressure drop( $\Delta p$ ) by along the tile, and the air density( $\rho$ ). This value considered as the perforation ratio in CFD simulation.

$$K = \frac{\Delta p}{0.5 \rho U^2} \quad (13)$$

Here, the momentum source method proposed by [28] to correct the momentum deficit can be calculated by

$$F_y = \frac{1}{V} \rho \dot{V} \left( \frac{\dot{V}}{\sigma A_{tile}} - \frac{\dot{V}}{A_{tile}} \right) \quad (14)$$

While  $F_y$  is the body force per unit in vertical direction  $V$  is the volume of the tile  $0.61 \text{ m} \times 0.10\text{m}$  [19],  $A_{tile}$  is the surface of the tile,  $\sigma$  is the perforation ratio of the tile. The correct mass flow rate is calculating by  $(\dot{V}/A_{tile})$ . The height of body force rethe gion is 0.10 m which is the height of the tile where the small jet is exiting from the tiles and produce the single large jet[24,27].

In [20] simulation setting for tiles, the mass flow rate of each tile which measured in his experimental study imposed in boundary condition [6], while in the current study the mass flow rate extrapolated by simulation calculation of Fluent. And nearly the same value was obtained. Note that in [20] study as the mass flow rate imposed to each tile consequently, the velocity profile at the surface exit of all tile is uniform, but in my study, since the mass flow rate is not imposed the velocity profile is not uniform. The measured mass flow rate of each tile and in table [6] calculated mass flow rate of each tile is presented [7].

Tile a	Tile b	Tile 1	Tile 2	Tile 3	Tile 4	Tile 5	Tile 6	Tile c	Tile d
0.24	0.29	0.28	0.31	0.32	0.33	0.32	0.32	0.31	0.32

**Table 6.** Measured mass flowrate( $\text{m}^3/\text{s}$ ) of the tiles [20]

Tile a	Tile b	Tile 1	Tile 2	Tile 3	Tile 4	Tile 5	Tile 6	Tile c	Tile d
0.25	0.28	0.29	0.31	0.32	0.33	0.33	0.32	0.31	0.32

**Table 7.** calculated mass flow rate in my study( $\text{m}^3/\text{s}$ )

## 2.5 CRAH modeling

CRAH is also modeled as hollow box according to the ANSYS user guide [29], the bottom and top of the box are open and 2 fans one on the bottom and one on top is modeled the top fan sucks the air in the room and the bottom fan push the cold air into the under-floor plenum, black box model approach considered to design the CRAH, so then what we don't have information in the CRAH also the equipment of CRAH such as condenser, pump,...) are not considered in designing.. the flow direction, mass flow rate of CRAH, and the supply temperature are imposed in the in simulation.

## 2.6 buoyancy and radiation effects

Bouyancy is the resulting force is conveyed by a fluid on the object which it is sunk or floating. The importance of the bouyancy effect studied by[20]. Bouyancy affect both on the distribution of cold air flow exiting from perforating tiles and exit of racks. Consideration of the bouyancy effect in CFD calculation requires solving the energy equation which requires around 30% percent additional computational time [30]. The importance of the bouyancy effect can be evaluated by Archimedes which is the factor used to estimate the importance of natural relative to force convection. The Archimedes number, Ar is expressed as:

$$Ar = \frac{\beta g L \Delta T}{U^2} \quad (15)$$

Where  $\beta$  is the thermal volumetric expansion coefficient of fluid ( $3.43 \times 10^{-3} K^{-1}$ ) for the air at 20°C [20], g is gradational acceleration ( $9.81 \frac{m}{s^2}$ ) L is defined as the vertical length and in this case is the height of the rack (2m),  $\Delta T$  is the average temperature difference between intake and exhaust of the servers ( $\sim 9.5$ ) and U is the characteristic of average velocity of preformatted tiles. If the Archimedes number is in more than the order of 1 or more ( $Ar > 1$ ), it means that the bouyancy is important and needed to be considered in the numerical simulation setting. If the  $Ar < 1$  it is obvious consideration of this effect in simulation is unless and takes less time for solving the numerical analysis. The effect of bouyancy model in ANSYS Fluent calculate the bouyancy force directly from the variation of density in the airflow. this case the bouyancy effect was more than 1 so, considered in the numerical setting. In current study, bouyancy is selected as flow condition in problem setting of software, and corresponding of bouyancy model, the effect of natural convection is also considered in this work.

According to the analysis of [18], the effect of heat transfers due to radiation for the hot surfaces of servers to the surface of walls, ceiling and floor in data center accounts only  $\sim 1\%$  that can be neglected in the data center CFD simulation settings.

## 2.7 Mesh generation and grid independent

For the present problem configuration, two different grid size is carried out in order to understand the effect of grid size the accuracy of the numerical solution and ensure grid independent results. ANSYS Icepak 15.0 version has different mesh generation setting respect to Gambit or mesh generator software of ANSYS Fluent. The comparison of temperature profile 0.3m in front and behind the racks was used to analyse the result of different mesh configuration to find the grid independent solution. Grid-independent solution is modeled on two different mesh size. coarse grid with 200mm maximum element size in X, Y and Z direction and the minimum gap size 0.001m has selected for X, Y and Z direction, unstructured hex mesh type is used, local mesh on object parameters are not applied in the first case, the in the global mesh parameter coarse mesh has selected and the value for minimum element allowable in gaps, the minimum element on edge the maximum ratio according to the [31] is chosen 2,1 and 10. No mesh O-grid has selected and the mesh assembly separately has checked in order to avoid the separation of mesh design in the model, also the in the option setting checked the allow minimum gap changes, this option is useful in situation that two surfaces with different boundary condition or different thermal characteristic set the minimum distance automatically in the surfaces so avoiding confusing in calculating the continuity, momentum and energy equation in the nodes. corresponding the setting mesh consist of 58399 cells. And in the second case fine grid size with maximum 102mm in X, Y and Z direction element and 0.001m again is chosen for minimum element size, the unstructured hex mesh type is used alike the coarse mesh the for the value of minimum element gap minimum mesh element on edges and the maximum size ratio is chosen 3,2 and 2 according to [31] , the other setting that applied on coarse mesh are applied in mesh refinement. Unlike the coarse mesh in refinement mesh, the local mesh on object parameters is used. this option in Icepak mesh generation setting allow to have a finer mesh in the surface of the objects that the thermal parameters have a significant variation, in the per-option parameter tool box there is possibility to choose the surfaces and the value in X,Y and Z direction that shows, the number in a certain direction states the number of division in a certain surfaces, by default the number is 1 it means respect to normal mesh configuration no changes is applied for example by choosing the number 4 in a surface that has 10 mesh size in Z direction correspondingly the number of mesh size in Z direction becomes 40. And

since the mesh assembly separately is active, the software tries to have balance in the concentrated and non-concentrated zone this comment is like the (inflation) option in Gambit mesh generator software. consequently, the perforated Tiles, Racks inlet and out the surface, CRAH supply and return surface are used. In **Fig. 11** the left photo in the first row is demonstrating the coarse mesh in addition to coarse grid size the on the is showing the option mesh assembly separately on the top and bottom of the rack. And in the second row the presence of mesh object per parameter in front, back of the rack and in the tiles is showing.

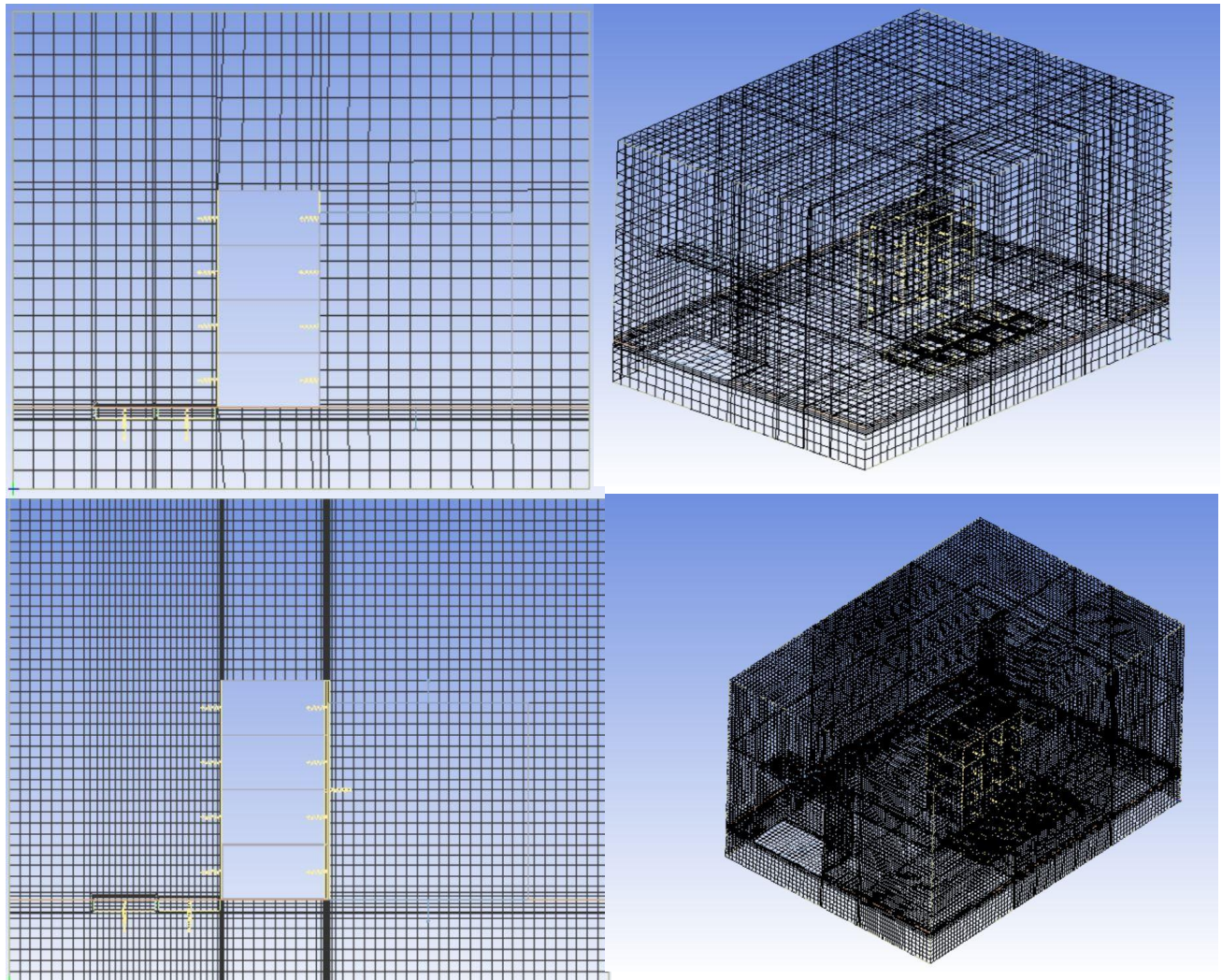


**Fig11.** Coarse grid (top) and fine configuration along Y-Z plane and 3D view

Corresponding to different mesh size, **Fig. 11** shows that there was not a major difference in temperature profile in Y-Z plane at 0.3m in front of the first rack since the temperature velocity and pressure do not have a significant difference in a data center along a different direction. It can be saying that in this model configuration the mesh size does not play an important role. In both mesh configuration same basic setting for simulation was applied, the maximum number of iterations set 500 and for the energy convergence criteria according to Icepak user guide [31] set 0.00001 and both for turbulent kinetic energy and turbulent dissipation rate convergence 0.001 value is applied. Both simulations have performed by Core-i7 CPU. in **Fig. 12** right photo is solution residuals for the coarse mesh configuration takes about 7 minutes and after 273 iterations is converged corresponding the setting convergence criteria, and on the left the solution residual for the mesh refinement configuration that takes about 35minutes and after 382 iterations is converged corresponding the same setting convergence criteria.

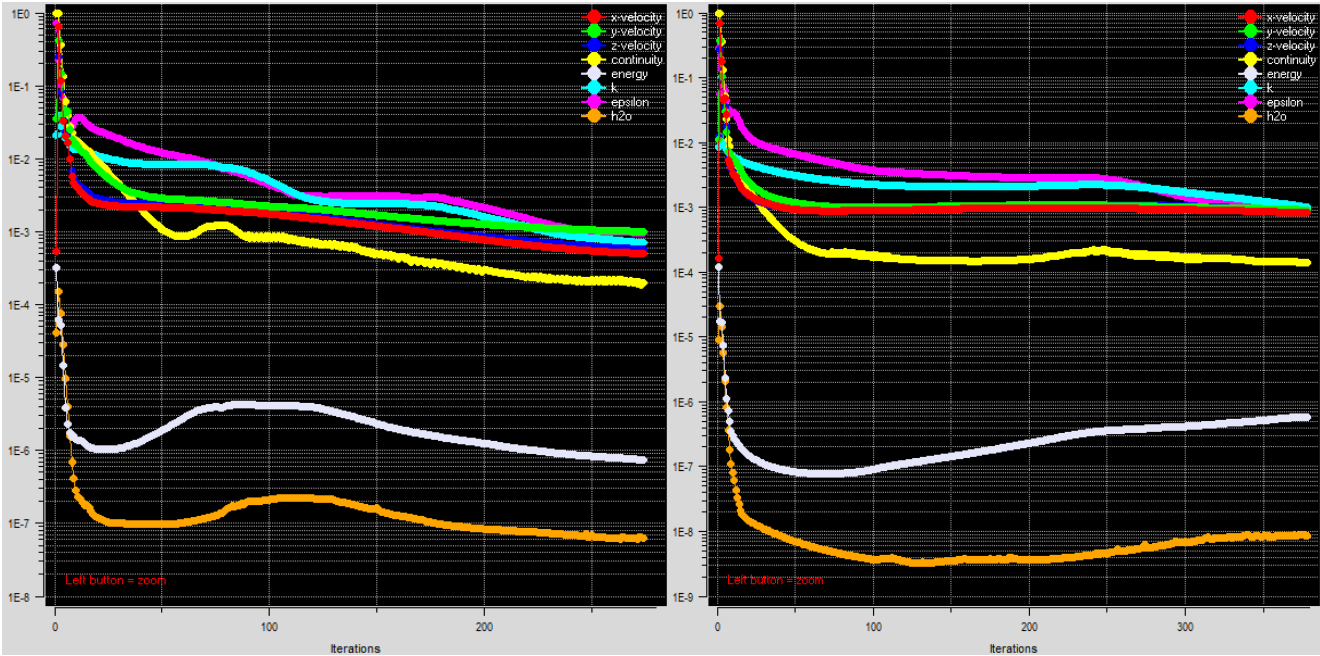


**Fig 12 .** Solution residual criteria for coarse grid (left) and fine grid (right)

## 2.8 Boundary conditions:

In the general setup for CFD simulation setting the flow (velocity and pressure) and the temperature is checked, since there is no source of radiation heat transfer, radiation is turned off. Flow regime in all the control volume is turbulent, for the effect of natural convection, gravity vector is checked and the  $(-9.81 \text{ m/s}^2)$  in the time variation steady state is selected, for the velocity initialization in simulation setting in X and Z direction 0 value selected and as the Fluent user guide recommended [31] the minimum value for the Y axis is selected  $(0.1 \text{ m/s})$ . for the effect of natural convection ideal gas law is chosen and the operating pressure 101kPa is considered, the same value of RH (60%) for the same ambient condition of ASHRAH diagram. All the surfaces of room considered adiabatic so there is no heat transfer to the outer part. In the **table 8**. the summary of the general setting and boundary condition is presented.

Parameters	value
R1 power	15kW
R2 power	15kW
R3 Power	15kW
CRAH 1 flow rate	3.04 m <sup>3</sup> /s
CRAH 2 flow rate	0
CRAH supply temperature	13°C
Tile opening ratio	25%
Rack Opening ratio	56%
Turbulence Model	Realizable k-epsilon
Wall & ceiling	Adiabatic
Leakage flow	Negligible
Radiation	off
Buoyancy	Yes

**Table 8.** General CFD boundary conditions

## 2.9 Grid study and validations

In this section the I present different CFD simulation with same boundary condition used [], CFD simulation results will be validated against the improved CFD case study of [20] and the steady - state data that measured with poles sensors in DC/RL. The temperature distribution profile of R1, R2, R3 in front and the rear side at the 0.3m front and back of the rack is compared. The three cases(A, B, C) analyzed with improved case k-epsilon turbulence model of [20] (D) and [20]the experimental data (E) in this chapter with:

- baseline CFD case Realizable k-epsilon turbulence model (A)
- Improved CFD case k-epsilon turbulence model (B)
- Improved CFD case Realizable k-epsilon turbulence model (C)

These three cases labeled as case A, B, C. Each rack heating power is ~15kW and ~1.32m<sup>3</sup>/s flow rate passed through its corresponding of ~9.5°C, the ratio of total tile airflow to total rack airflow is 0.76. The details value of measurement airflow of the rack is specified in the boundary condition of each rack chassis in CFD simulation. Under the steady-state condition, CRAH supply temperature set at 13°C and the mass flow rate was 3.04m<sup>3</sup>/s(downward to the under-floor plenum. The average temperature of inlet CRAH measured by sensors is ~25.7°C considering as reference [20]. The CRAH average temperature calculated by different scenario (case A, B, C) 25.08°C, 24.96°C and 25.12°C (less than 5% error respect to reference temperature. A simple energy balance in CRAH supply and exhaust temperature and heat rack power generation can verify that a general simulation model designed correctly.

$$\dot{Q} = \dot{m}c_p\Delta T \quad (16)$$

$\dot{Q}$  is the power of CRAH and  $\dot{m}$  is the mass its mass flow its rate (rack and CRAH1)

Case	Grid size (mm)	Chassis BF	Tile Bf
A	200	No	Yes
B	102	Yes	Yes
C	102	Yes	Yes
D	102	Yes	Yes

**Table 9.** Gridding size and body force consideration in the different study

Beginning with A case which has the same configuration of the center and k-Realizable turbulence model. In the next step the same turbulence model that [20] used in his simulation will use and compare with Realizable-k epsilon turbulence model that I proposed according to the [Fluent user guide], and then in following step improve the CFD model until reaching “best” case study, focusing on the mesh size and mesh parameter with the boundary condition of was performed .

**baseline CFD Realizable k-epsilon turbulence model (A).** the current model is chosen based on [20] the experimental information, his CFD simulation, and recent literature studies and Ice Pak user guide [31] and ANSYS fluent user guide [30].

- A coarse grid with the maximum cell size of with 200mm.unlike Gambit mesh generator software that also allowed larger cell size created in Icepak ANSYS 15.0 mesh generator doesn't allow any cell created larger than defined cell size.
- A recently developed standard k-epsilon model (Realizable k-epsilon) turbulence model is chosen [21]. The boundary condition of turbulence quantiles chosen based on recommended values of ANSYS Icepak 15.0 user guide [31](academic version) commonly used in data center CFD simulation.
- Bouncy and natural convection effect are considered as proposed recent CFD publication for data center simulation [20].in parametric study nearly similar value for Ar obtained, [20] found that the bouncy effect is important to be considered in setup and test condition of DC/RL facility. Bouncy effect consideration helps to have better perdition in thermal properties at the outlet and inlet perforation surfaces. In this case better predication profile at the inlet of Racks.
- flows velocity at the inlet of Racks and outlet (supply) CRAH are modeled as uniform velocity. While the tile velocity profile is not imposed and extrapolated from numerical computation.
- The under-floor plenum is modeled is not modeled by [20] unlike in this study and considered no leakage and at the tile's adages and CRAH intersection to the under-floor plenum.

The A case employs a coarse grid but with consideration of edges and objects intersections, but no object mesh refinement consideration, with maximum (200mm×200mm×200mm) in the entire domain. Coarsening of the mesh sized, the total number of cells obtained was 58399. In table []

summarized the general boundary condition of the case (A) CFD simulation. as in this case used coarse mesh grid, the large-scale gaps at the edge of the rack doors and CRAH(s) are not modeled. The temperature profile along the center line of the tiles (T1, T3, T5) front of the Rack( R1, R2, R3), (R1 is the closest rack to CRAH1, R2 is the middle and R3 in farthest Rack from CRAH1 and )and 0.3m behind the same racks is showed in **Fig 13** black continues line represent the case (A) CFD simulation and (E) line represent measured data with pole sensors in experiment study of [20]. As the tile temperature difference along its height the effect of bouncy is insignificant. Tile temperature considered as the reference temperature in [20] studied as he did not design the under-floor plenum and consequently the supply flow of CRAH, in current study CRAH supply temperature considered as a reference and while the temperature increment in the plenum is negligible, it does not make difference. The heat produced in under plenum cables makes may make some small difference. The temperature error between the case (A) study and case (E) at 1m, 2m, and 3.5m height are presented **table 10** and the temperature diagrams shown in **Fig13** until three quarter height of the front rack the (A) case study were had the same temperature profile respect to experimental test and [20] simulation. case A respect to experimental data has a notable error in of  $\sim 2^{\circ}\text{C}$  less temperature gradient at the top server racks, will test data show less diffuses much more mixed temperature filed. Note that the temperature near the tile region doesn't influenced by recirculation effect and remained the same value of tile temperature. above, or on the other word due to the 'potential core' of jet flow which is coming from the tiles the temperature at the lower server remain near to the tile temperature. Case A simulation shows that the temperature will arrive maximum to  $25^{\circ}\text{C}$  at the top of the first rack will the test data shows that will arrived up to  $27^{\circ}\text{C}$ , while this value in [20] simulation study shows that it will arrive up to  $18^{\circ}\text{C}$  that a significant difference respect to test experience. These difference can also be seen in the temperature field in a vertical plane cut in **Fig.14** in front of the R1.**Fig 14** also shows in A case of study the flow at the entrance of the rack and the region between the wall and racks is wider and spreader more respect the test value while in [20] simulation the flow entered in the rack are sharpened. Fig shoes that fronted racks have  $\sim 2^{\circ}\text{C}$  and rear racks have  $\sim 1^{\circ}\text{C}$  difference respect to the test data. The temperature rises across the chassis centerline **Fig. 13** in three cases (A, D, E) while in A case predicted a lower temperature respect to test data while in (D) case study predict the lower temperature

<b>Front</b>	<b>Rack3</b>	<b>Rack2</b>	<b>Rack1</b>
H = 1 m	0	0.35	-0.3
H = 2 m	-2.05	-2.5	-1.2
H = 3.5 m	-3	-2.2	-1.5
<b>Back</b>	<b>Rack3</b>	<b>Rack2</b>	<b>Rack1</b>
H = 1 m	-0.1	+0.3	-0.8
H = 2 m	-1	-0.5	0
H = 3.5 m	-1.35	-0.7	-0.4

**Table 10.** Error (°C) in front and behind the rack for case (A)

**Improved CFD case k-epsilon turbulence model (B).** Also, this work based on the same boundary condition that obtained in an experimental test of [20], and Ice Pak user guide ANSYS 15.0.

- A fine grid with a maximum cell size of with 102mm and mesh refinement used in inlet and outlet of the racks and CRAH 1, perforation tiles in, case B, in Ice Pak ANSYS there is an option in mesh generating setting to specify the mesh refinement for selected objects and surfaces. By choosing the value more than 1 Object-Specific Meshing Parameters [31], count the number of the mesh used in normal case of meshing and multiply it by the value specific, (e.g. by choosing the value in 6 for the vertical direction of tiles, the number of grid in vertical line which was 2, arrives at 12. More accurate information about thermal properties will obtain.
- A standard two equation of k-epsilon turbulence model selected in the current study (same turbulence model used [20], to understand with the difference of [20] study with ANSYS

13.0 Fluent and ANSYS Icepak 15.0 simulation. (note that the detail information of CFD setting of the author is not available)

- The values for difference of temperature at the inlet and outlet of the racks and CRAH, and velocity of the tiles were nearly the same, nearly the same value for Ar is obtained (1.4). consequently, like the previous simulation setting buoyancy effect is considered.

The case (B) employs fine mesh and in addition consideration of edges and object intersections, considered object per parameter in extra refinement with a maximum grid size of 102mm×102mm×102mm in the entire domain. 393538 total number of cells, (nearly 8 times more than case (A) study) obtained with refinement mesh in the room. in **table 8** showed the general boundary condition of the case (B). the large scale- the gap is considered in the rack, CRAH and tile opening. Different object parameter number is chosen according to in X, Y and Z axis direction for each surface. The momentum source both in tile perforation and rack exhaust door by adding two opening thin surfaces modeled in this study. Rack percentage of porosity considered 56% as proposed by [20]. Like the previous study the temperate temperature profile along the center line of the tiles (T1, T3, T5) front of the Rack( R1, R2, R3), (R1 is the closest rack to CRAH1, R2 is the middle and R3 in farthest Rack from CRAH1 and ) and 0.3m behind the same racks is showed in **Fig 13**..line represent the case (B) CFD simulation an compared with tested temperature profile. the results show that in case (B) CFD simulation respect to case (A) doesn't have a significant difference in the temperature profile. The detail of error at the height of 1m,2m, and 3.5m with respect to experimental data is shown in table 11.

<b>Front</b>	<b>Rack3</b>	<b>Rack2</b>	<b>Rack1</b>
H = 1 m	1.9	0.9	0.4
H = 2 m	-3.2	-2.8	-0.2
H = 3.5 m	-1.8	-0.7	0
<b>back</b>	<b>Rack3</b>	<b>Rack2</b>	<b>Rack1</b>
H = 1 m	-0.85	1.8	0
H = 2 m	3.2	0	0
H = 3.5 m	1	-0.6	0

**Table 11.** Error (°C) in front and behind the rack for case (B)

**Improved CFD case Realizable k-epsilon turbulence model (C).** Also, this case based on the same boundary condition that obtained in an experimental test of [], and Ice Pak user guide ANSYS 15.0.

- The same configuration of mesh generation setting of the case (B) is applied in the current case.
- Like the Case (A) study, developed of the standard k-epsilon model (Realizable k-epsilon) turbulence model is chosen [21]. The boundary condition of turbulence quantiles chosen based on recommended values of ANSYS Icepak 15.0 user guide [31](academic version) commonly used in data center CFD simulation.
- As the configuration and velocity and temperature equipment were nearly the same as the other cases, so bouncy effect in this case also considered. As it is showing in **Fig. 13** and **table 12** the temperature profile of the front and behind the racks the minimum error respect to the previous simulation.

<b>Front</b>	<b>Rack3</b>	<b>Rack2</b>	<b>Rack1</b>
H = 1 m	0.6	1	0.1
H = 2 m	-0.8	-1.35	0
H = 3.5 m	-0.85	-0.55	-0.25
<b>Back</b>	<b>Rack3</b>	<b>Rack2</b>	<b>Rack1</b>
H = 1 m	-0.85	1.5	-0.15
H = 2 m	-0.75	0	0
H = 3.5 m	1	-0.55	-0.5

**Table 12.** Error (°C) in front and behind the rack for case (C)

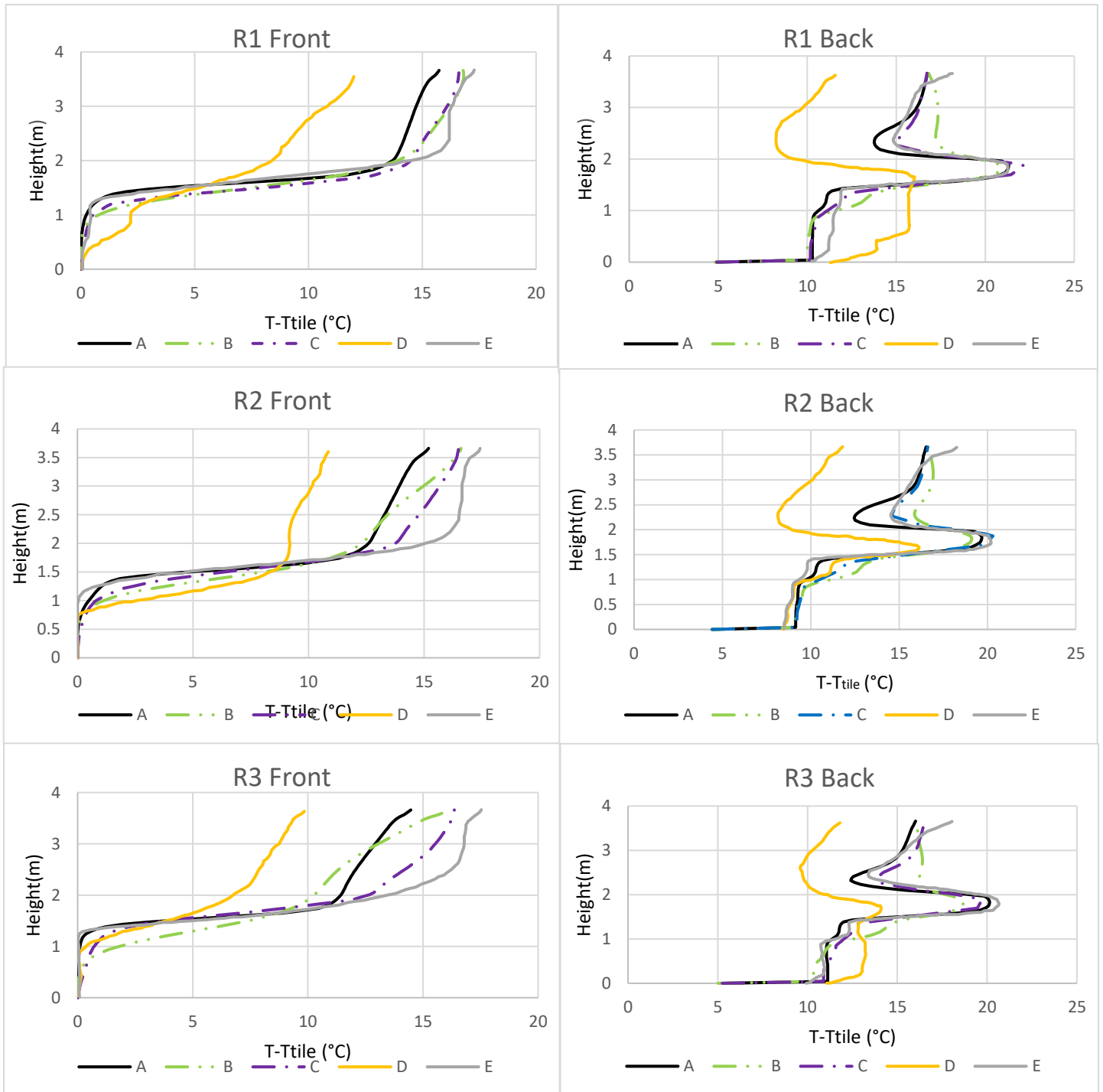


**Fig 13.** Comparison of temperature distribution at the 0.3m from inlet and outlet of racks at front in vertical direction (baseline k- Realizable turbulence model: case (A), Improvement k-Epsilon turbulence model :case (B), Improvement k-epsilon turbulence model: case (C), Improvement k-Epsilon turbulence model of [20] : case (D) , Test data Case (E)[20]

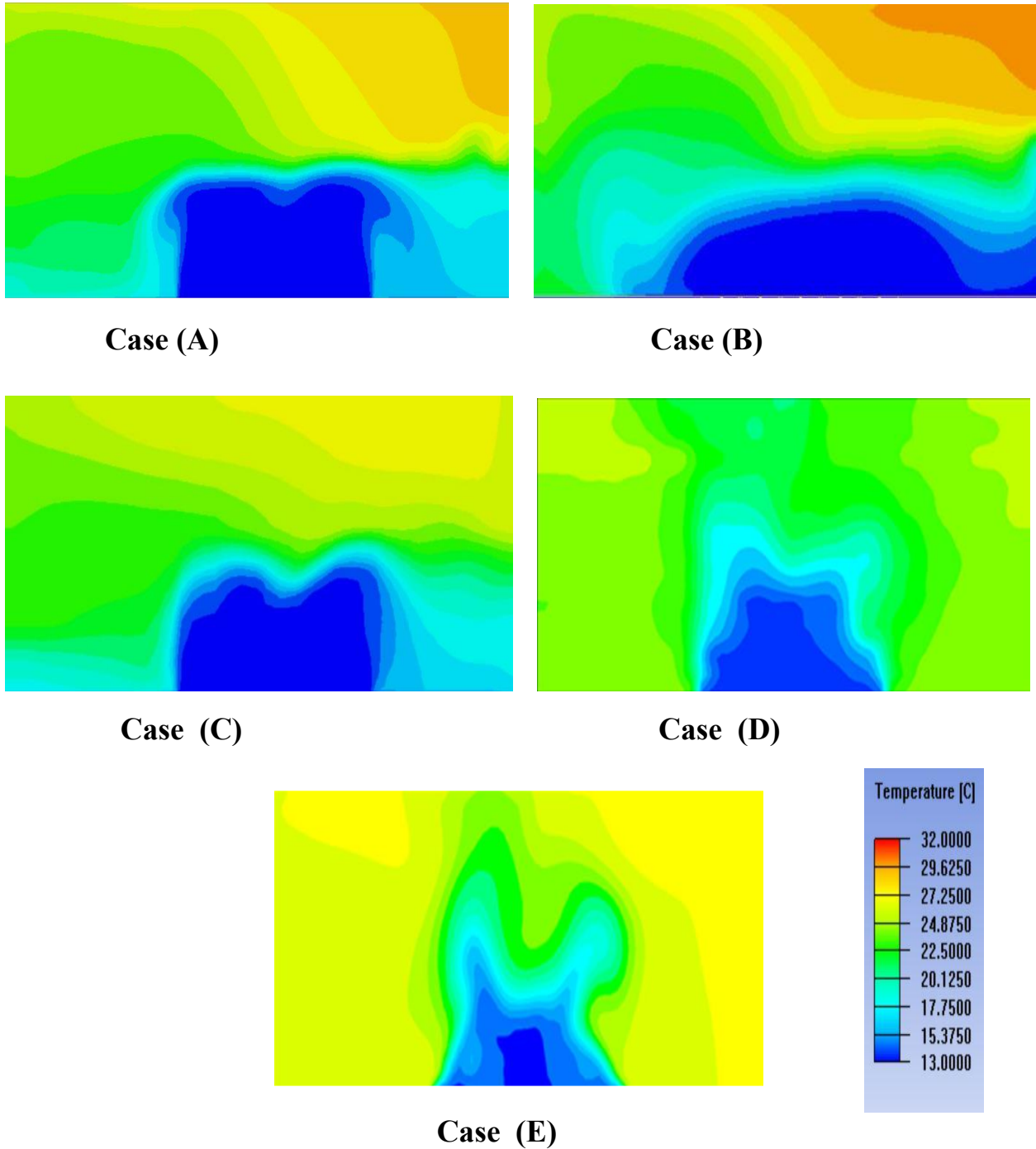
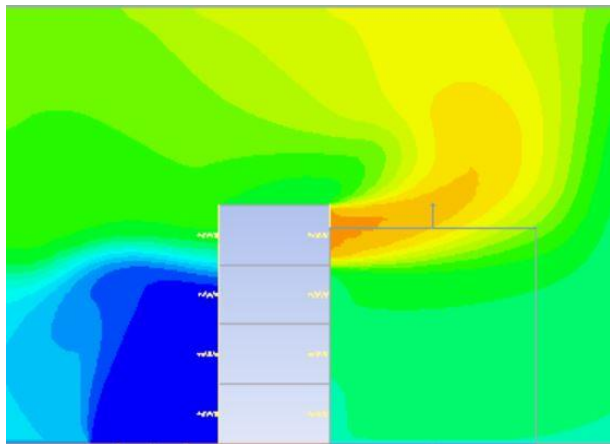
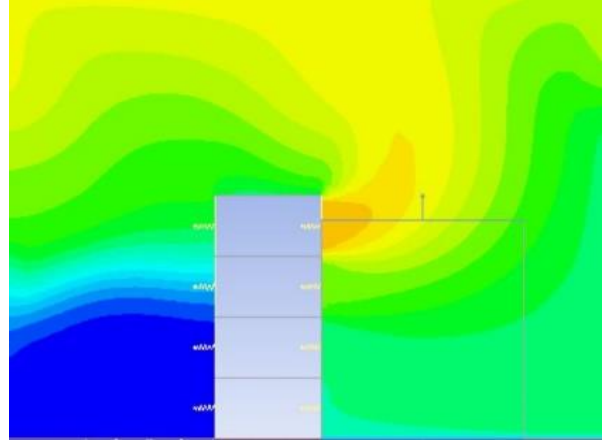


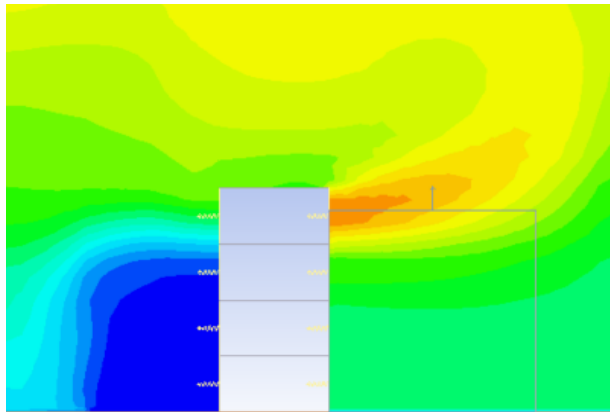
**Fig 14.** Comparison of temperature contours in Y-X plane at 0.3m in front of the racks (baseline k- Realizable turbulence model: case (A), Improvement k-Epsilon turbulence model :case (B), Improvement k-epsilon turbulence model: case (C), Improvement k-Epsilon turbulence model of [20] : case (D) , Test data Case (E)[20]



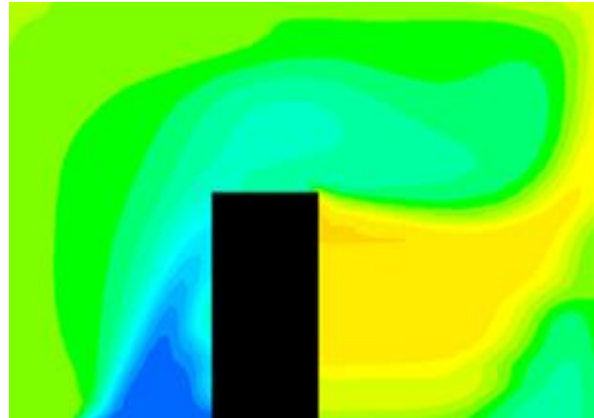
Case (A)



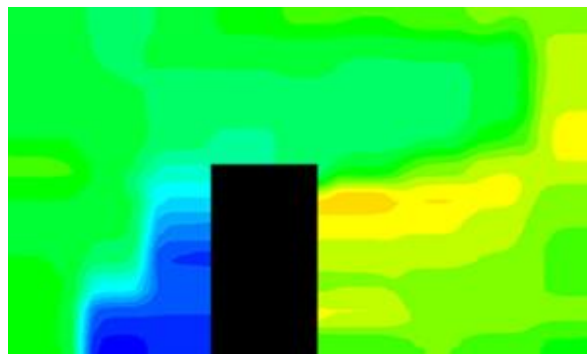
Case (B)



Case (C)



Case (D)



Case (E)

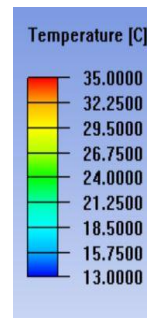


**Fig 15.** Comparison of temperature contours in Y-Z plane at the middle of the R1 (baseline k-Realizable turbulence model: case (A), Improvement k-Epsilon turbulence model :case (B), Improvement k-epsilon turbulence model: case (C), Improvement k-Epsilon turbulence model of [20] : case (D) , Test data Case (E)[20]

## Chapter 3

### Energy efficiency of data center

#### 3.1 Thermal metrics analysis

In order to evaluate a data center thermal performance, several non-dimensional parameters are proposed. Thermal metrics play a very important to operate the data center with high energy efficacy and reliability, reliability is the most important objection in the data center. There are five parameters interduce in chapter 1. In the current study we analysed the extrapolating data in Icepak ANSYS 15.0 report. These indices are listed with their evaluation priority

- Rack cooling index ( $RCI_{Hi}$ )
- Rack cooling index ( $RCI_{LO}$ )
- Return index (RTI)
- Supply heat index(SHI)
- Return heat index (RHI)

Reminding that rack cooling index parameter based is on the temperature distribution along the rack height, rack cooling index can express in two limitations  $RCI_{Hi}$  and  $RCI_{LO}$ , are evaluating by the ASHRAE diagram recommendation temperature range. **Fig. 5.**

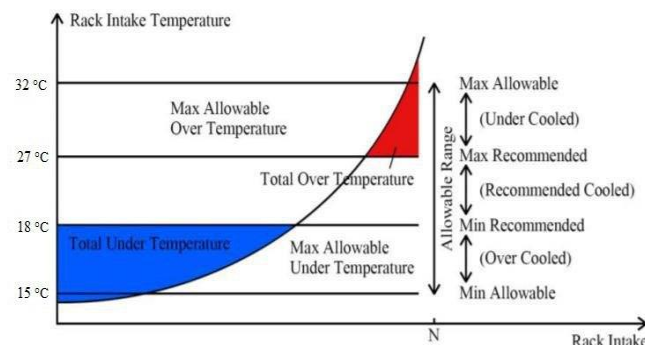


**Fig 5 .** Definition of total over-temperature and total under temperature

And Return temperature index is concerning about the level of bypass and recirculation, is the ratio of the temperature difference in supply and return of CRAH over the average temperature of inlet and exit for each rack. and SHI and RHI are concerning about the efficacy of the airflow in the racks.

In the previous chapter, we provide a different case of study for validating the CFD analysis against the experimental data. The temperature profile along the vertical axis of R1, R2 R3 didn't have a significant difference in different case of study, however in the current study I use the value obtained from summery report of CFD simulation, the information about the mass flow rate of each server rack and CRAH and also the return and supply temperature is available but unfortunately, the experimental test data for the intake and outlet of server are not available. In current parametric calculation, the temperature of CRAH inlet is 13°C, the same value in test experimental data, CRAH average return temperate is 25.08°C while the average temperature in the experimental study of [20] 25.7°C (2% error). In the **table13**. the average supply and return temperature of each server from the Ice Pak report is shown. Note that Rack1 is the closet rack to CRAH and the row each two values are belonging to one server rack. and starting from the bottom server. [20] mentioned that the average temperature difference for the racks is ~9°C, also in the current simulation the same data obtained by the CFD report of simulation.

Rack N	Supply	Return	Supply	Return	Supply	Return	Supply	Return
R1	13.44	22.60	13.70	23.15	15.70	25.25	24.82	33.23
R2	13.04	22.20	13.35	22.76	16.34	25.28	24.56	32.45
R3	13.88	23.59	14.54	24.38	16.21	26.01	22.96	32.01

**Table 13.** Average supply and return temperature servers by  $T_{Ref}$  13°C (from bottom to top in horizontal line)

As it is observing in **table 13**. the coldest server rack is located at the middle of the first row and its temperature is near to the tile temperature and the hottest server rack is located at the fourth row of the R1, as the nearest rack has the minimum airflow rate, the temperature augmentation is

observing more than other chassis, the air velocity direction in front of the rack is counterclockwise, so the direction of air recirculating slightly influence on the temperature of the server racks. The first chassis of R3 is influenced more than R2 and R3, so in all scenarios in the first row R3 has the warmest temperature. in the second row of the rack still, the second server has the minimum value and the third one has the maximum value. and the reason is that middle server has the maximum value of mass flow rate and still air effect of air recirculation does not have significant effect on the inlet temperature , in the third row of the racks the effect of air recirculation is more evident, all the temperature areas it was expecting increasing, unlike the first and second row of the server in the third row the middle rack has the maximum value and the R1 has the minimum value, the justification of this-this issue is that the increasing of mass flow rate of the server, and the mass flow rate is taken by the middle server rack is coming from the air recirculation from side and upper part of the racks. The fourth row of the server this scenario is changing, and the first server has the warmest server rack and this issue can be justified with the effect of air recirculating and the direction of velocity vectors. The middle top server has the highest air mass flow rate of  $0.37(\text{m}^3/\text{s})$  and for R1 and R2 are  $0.31(\text{m}^3/\text{s})$ .

According to the study of [32],  $\text{RCI}_{\text{Hi}}$  has the most priority for evaluation in thermal metric parameters as avoiding the over temperature in server racks not only cause more power consumption but also may cause irretrievable damage. Typically, the fourth row of servers is sensible for this metric, as it is showing in **Fig. 16**, the intake temperature of R1, R2 and R3 are  $24.82^\circ\text{C}$ ,  $24.56^\circ\text{C}$  and  $22.96^\circ\text{C}$  and the recommended temperature according to the ASHRAE thermal guideline is  $27^\circ\text{C}$  all three racks have lower value respect to the maximum recommended temperature so definitely a risk of overheating does not thread the rack servers. The maximum recommended and the allowable average temperature for server inlet according to [12]  $27^\circ\text{C}$ ,  $32^\circ\text{C}$  in A1 class which is according to the classification of ASHRAE is suitable for the normal data centers.as it is showing **Fig. 16**  $\text{RCI}_{\text{Hi}}$  100% is an ideal value for the current metric. Top servers' chassis which more sensible to this value has the temperature  $\sim 4^\circ\text{C}$  less than the recommended maximum temperature of ASHRAE.

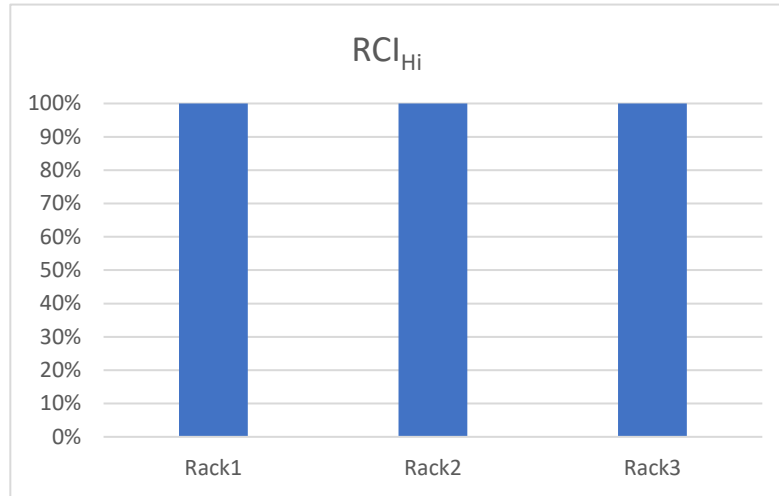


**Fig. 16.** RCI<sub>Hi</sub> (%) by T<sub>Ref</sub> 13°C

RCI<sub>Lo</sub> is the secondary important value according to the classification of [32], a high value for this parameter represent the absence of over-cooling, the consequence of low value of this parameter is wasting energy in the data center. Typically, in a high-power data center, the first and second row of chassis are a victim of reduction of this metric since the temperature of the racks increases suddenly in third and fourth rows of the rack. in this scenario, since supply temperature is significantly low not only the first and second row of serves are bellowed the but also the third row of servers are below the recommended value, and only the fourth row of servers are beyond the minimum recommended temperature according to ASHRAE thermal guideline. However, typically HVAC engineers of data centers are conservative, and RCI<sub>Lo</sub> value is lower than normal acceptable range **Fig. 5** Reminding that minimum allowable average temperature for the server inlet is 15°C and the recommended value for A1 class is 18°C **Fig 4**.

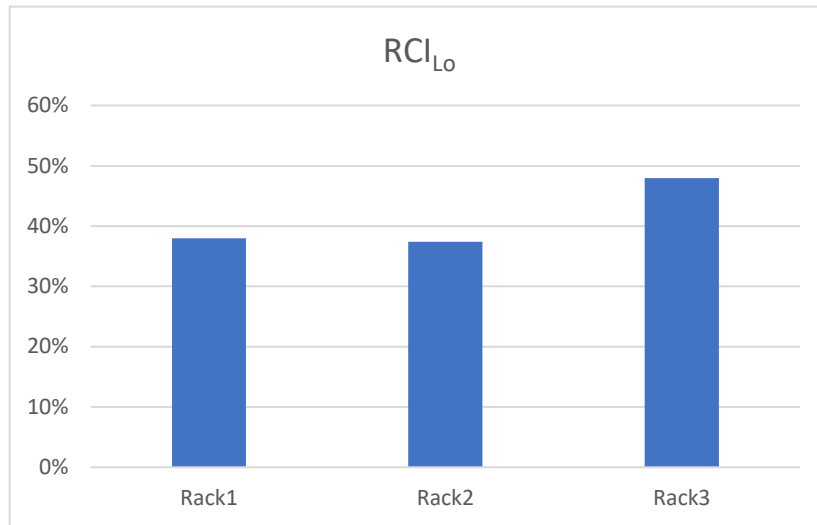


**Fig. 16.** RCI<sub>Lo</sub> (%) by T<sub>Ref</sub> 13°C

The third important thermal metric parameter is RTI, the value shows the level of bypass or recirculation which both are unpleasant factors in the data center. Reminding that this value can obtain by the average temperature difference of return and supply of the CRAH1 over the average temperature difference of inlet and outlet of each rack. presence of bypass and recirculating can be observed inside view of temperature plane-cut in **Fig. 15**. As it is showing in the third quarter of the rack (fourth row servers) the temperature counter is demonstrating higher value, it is because of the presence of warm air recirculating while if the temperature contours the presence of low temperature filed over the rack it means amount of supply temperature passing over the rack server and the flow is bypassed, and RTI value has a lower value than 100%. In the current study, it is clearly demonstrating from **Fig. 17** the presence of air recirculating. Average CRAH temperature calculates in Icepak report was 25.01°C. and as it is showing the R3 has the minimum RTI value that means lowest temperature difference of inlet and exist rack and the middle rack has the highest value of reciliation, the temperature difference of first and second row of R2 server was significant while in the third and especially fourth row this value was relatively high. As it is mentioned the general direction of the velocity vector in front of the rack is counterclockwise and that's the temperature difference of inlet and exit in the third rack has the minimum value.

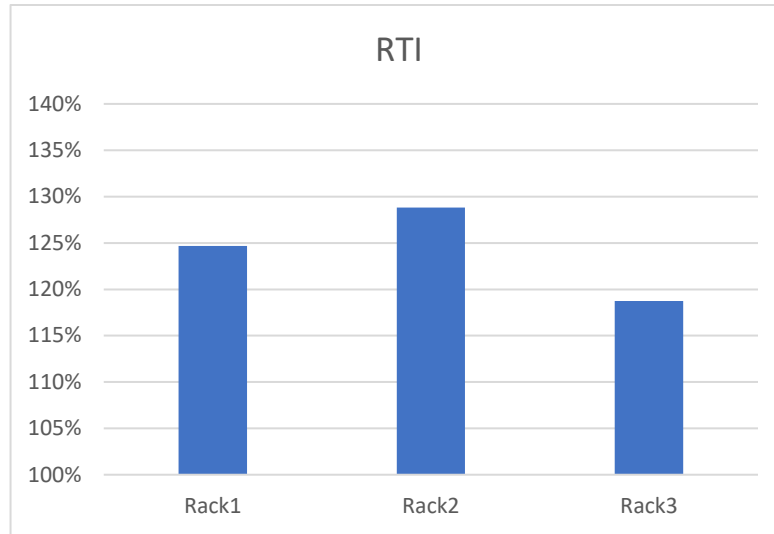


**Fig. 17** RTI (%) by  $T_{Ref}$  13°C

Generally, SHI and RHI values present air flow efficiency[32]. SHI value shows the air recirculation of cold aisles [33] and RHI is the ratio of the total heat extracted by the CRAH unit to the sensible heat gain by the server racks . These values are complementary of each other the summation of them is equal to 1. Ideal value for SHI is 0 so for RHI 100% in data centers. Which is difficult to archive. value less than 20% for SHI and more than 80% for RHI is the good value. In **Fig 18,19**, the parametric calculation for SHI and RHI are presented, these value for each rack shows the data center airflow are proportional.

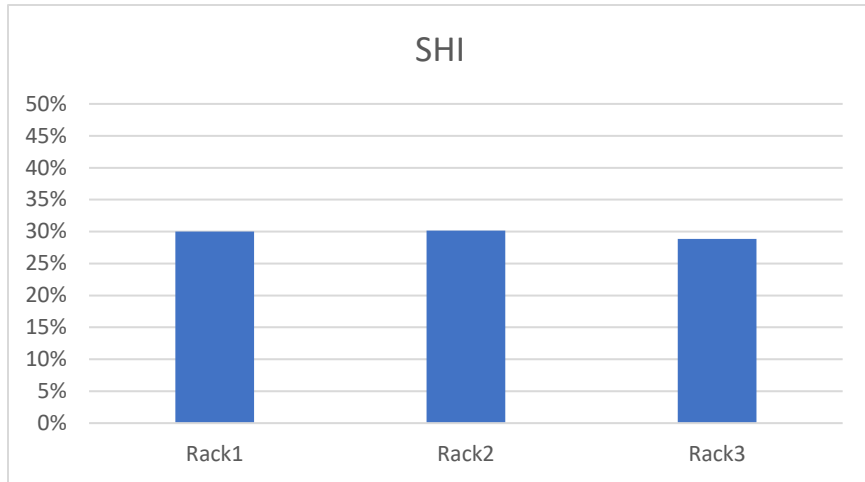


**Fig.18** SHI (%) by  $T_{Ref}$  13°C

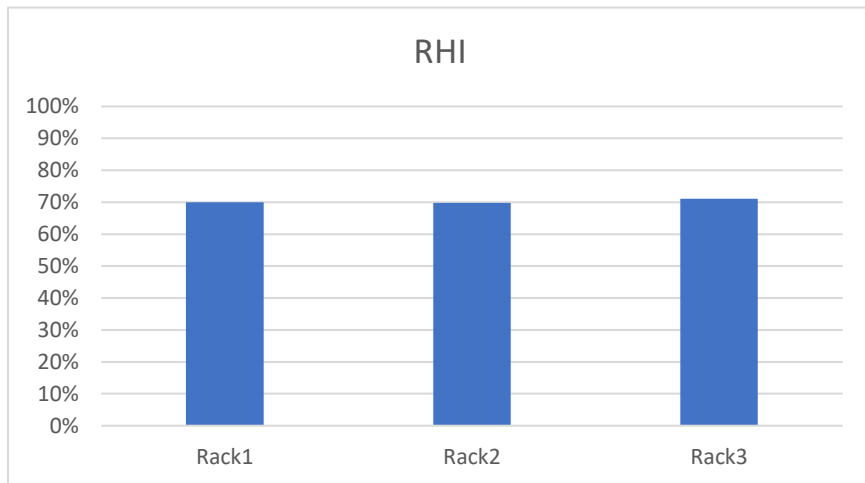


**Fig.19** SHI (%) by  $T_{Ref}$  13°C

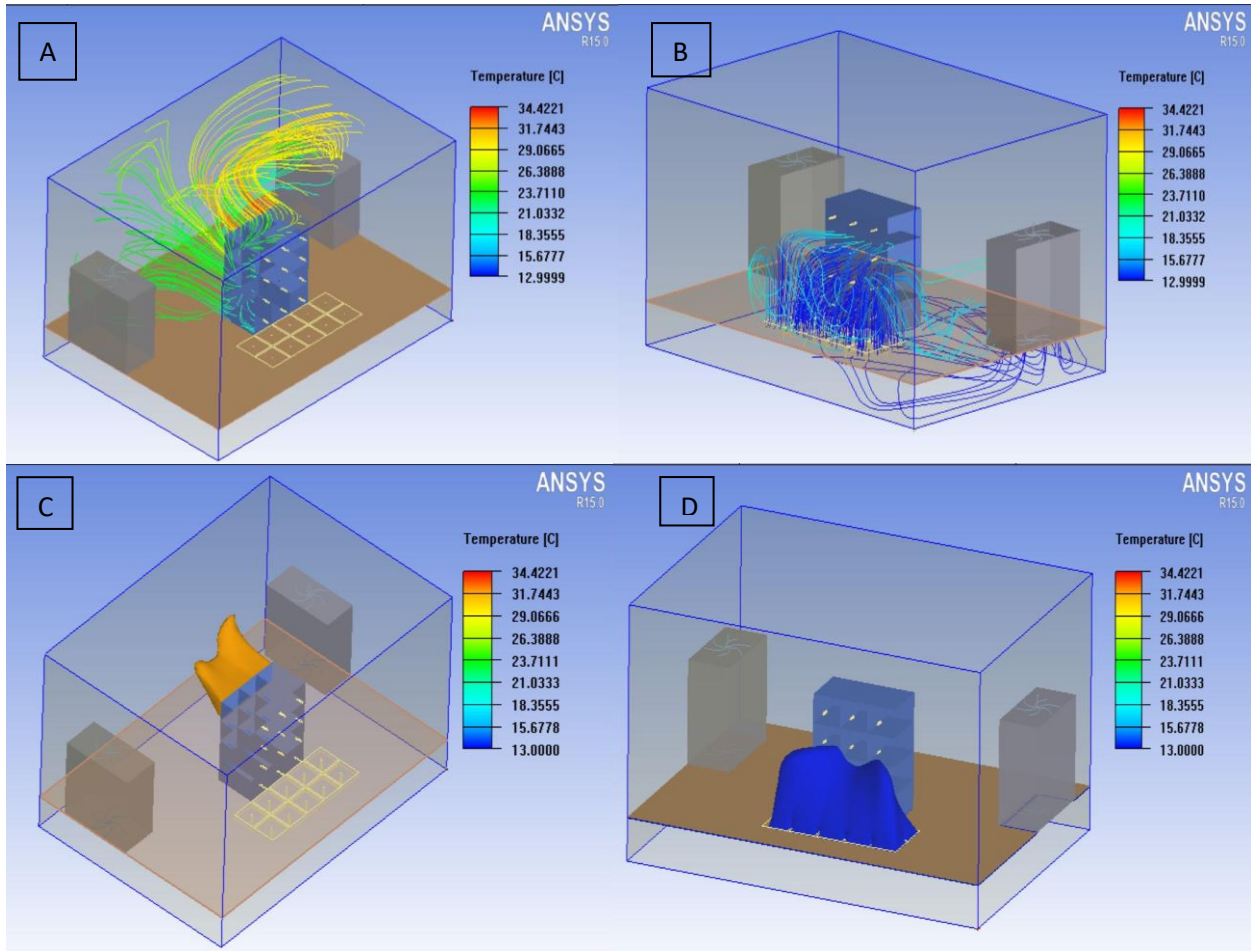


**Fig 20.** A: Return air path B: Supply air pass C: High-temperature clouds D: Low-temperature cloud

### 3.2 Supply CRAH temperature optimization

As the report shows they HVAC DC/RL was very conservative in choosing CRAH1 supply temperature,

according to ASHRAE thermal guideline [12] for minimum temperature recommended for inlet of the rack is 18°C, and the minimum allowable temperature is 15°C. 9 out of 12 racks are not only are below the recommended value but also under the allowable minimum temperature. The second important metric parameter [32] for evaluation of a data center thermal efficiency is the  $RCI_{lo}$  which by choosing the value 13°C for supply temperature this efficiency is very poor. In this part, I will choose different logical supply temperature to see its influence on different thermal metrics. Inlet and outlet temperature of each server rack by considering different supply temperature (13°C, 15°C, 16°C, 17°C and 18°C) of CRAH is presented in **Table 13, 14, 15, 16,17.**

Rack N	Supply	Return	Supply	Return	Supply	Return	Supply	Return
R1	13.44	22.6	13.7	23.15	15.7	25.25	24.82	33.23
R2	13.04	22.2	13.35	22.76	16.34	25.28	24.56	32.45
R3	13.88	23.59	14.54	24.38	16.21	26.01	22.96	32.01

**Table 13.** Average supply and return temperature servers by  $T_{Ref}$  13°C (from bottom to top in horizontal line)

Rack N	Supply	Return	Supply	Return	Supply	Return	Supply	Return
R1	15.43	24.57	15.68	25.13	17.7	27.24	26.58	35.02
R2	15.02	24.17	15.29	24.69	18.19	27.14	26.24	34.13
R3	15.89	25.6	16.51	26.34	18.09	27.9	24.68	33.72

**Table 14.** Average supply and return temperature servers by  $T_{Ref}$  15°C from bottom to top in horizontal line)

Rack N	supply	return	supply	return	supply	return	supply	return
R1	16.42	25.56	16.65	26.1	18.64	28.19	27.42	35.87
R2	16	25.15	16.23	25.63	19.13	28.08	27.12	35.02
R3	16.89	26.59	17.48	27.31	19.02	28.83	25.56	34.6

**Table 15.** Average supply and return temperature servers by  $T_{Ref}$  16°C (from bottom to top in horizontal line)

Rack N	supply	return	supply	return	supply	return	supply	return
R1	17.41	26.53	17.62	27.06	19.59	29.13	28.27	36.72
R2	17.01	26.11	17.15	26.56	20.1	29.03	28.02	35.91
R3	17.87	27.57	18.46	28.28	19.96	29.77	26.43	35.47

**Table 16.** Average supply and return temperature servers by  $T_{Ref}$  17°C (from bottom to top in horizontal line)

Rack N	supply	return	supply	return	supply	return	supply	return
R1	18.38	27.5	18.55	28.01	20.72	30.25	29.47	37.92
R2	18.02	27.07	18.08	27.5	21.16	30.09	28.94	36.84
R3	18.85	28.55	19.41	29.24	20.97	30.79	27.33	36.36

**Table 17.** Average supply and return temperature servers by  $T_{Ref}$  18°C (from bottom to top in horizontal line)

### 3.3 Rack cooling heat indices

As we mentioned before  $RCI_{Hi}$  is the most important parameter for evaluation in data centers. The numerical calculation values for  $RCI_{Hi}$  shows as it shows in **Fig. 21** the value for this parameter by choosing the supply temperature of 13°C and 15°C is 100% which is the target. This value for supply temperature of 16°C will decrease a little for R2, and the reason is the effect of the recirculation is more respect R1 and R3, But the value is near to the target value. at 17°C as top 3 upper racks are slightly over the temperature of recommended by ASHRAE and finally the at 18°C only their rack is in range of acceptable value for  $RCI_{Hi}$  while R1 and R2 are not, the reason that sided racks has a respectably better value for  $RCI_{Hi}$  is the presence of 4 sided tiles and that the decrease the influence of air-recirculating that coming from top and lateral part or racks. Choosing 18°C for RAH supply temperature may increase the risk of server failure, however reminding that the minimum  $RCI_{Hi}$  is 91% present which is equal to first rack value for  $RCI_{Hi}$ .

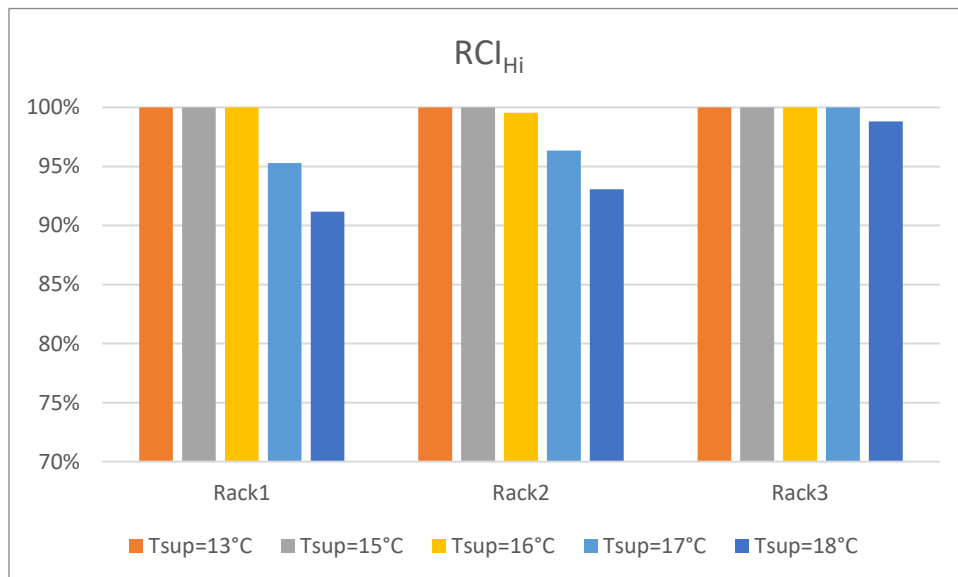


**Fig 21.**  $RCI_{Hi}$  (%) by  $T_{Ref}$  13°C,15, °C,16°C,17°C,18°C

Reminding that, the secondary important value for evaluation of thermal performance of data center is  $RCI_{Lo}$ , and low value for this parameter demonstrate energy waiting, or in the other word low temperature at the entrance of servers respect the recommended temperature of ASHRAE. As it shows in **Fig. 16**.  $13^{\circ}\text{C}$  is a very low temperature for CRAH supply,  $RCI_{Lo}$  increases by increasing the supply temperature only  $17^{\circ}\text{C}$  and  $18^{\circ}\text{C}$  values for the current data center are in the range of good temperature design temperature. However, usually, this value is lower than the acceptable range since safety has more priority respect to energy saving. **Fig 21** is showing the  $RCI_{Lo}$  value in different CRAH supply temperature.

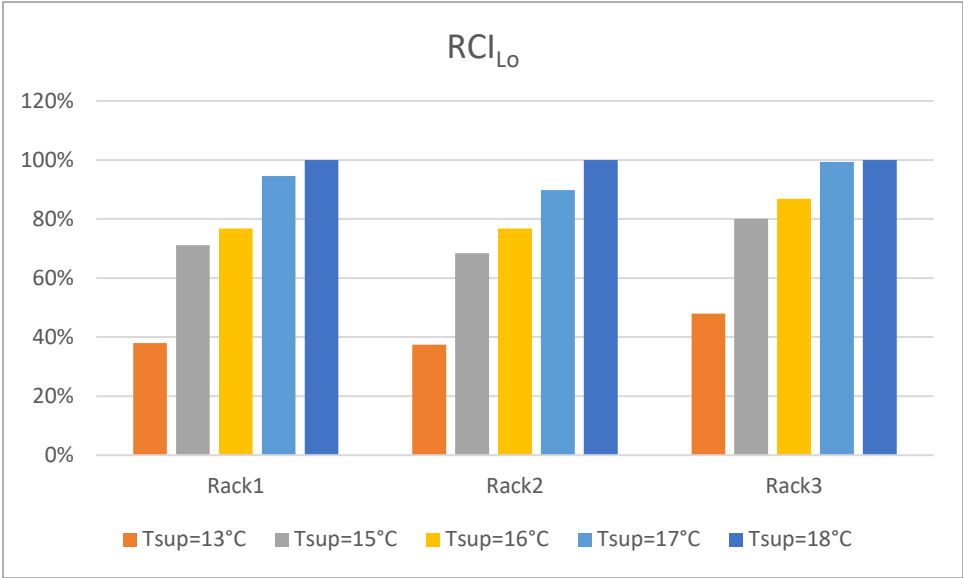


**Fig 22.**  $RCI_{Lo}$  (%) by  $T_{Ref}$   $13^{\circ}\text{C}, 15, ^{\circ}\text{C}, 16^{\circ}\text{C}, 17^{\circ}\text{C}, 18^{\circ}\text{C}$

### 3.4 Return Temperature index

Return temperature index which implies the value for air recirculation and by-pass air in the third important parameter for evaluation of data center thermal performance. The best value would be a temperature difference of supply and return CRAH of  $\sim 10^{\circ}\text{C}$  while [34] the best difference temperature for intake and exhaust of rack is  $10.19^{\circ}\text{C}$ . as it is showing [fig]the highest value for all different CRAC supply temperature is for R2, that are more victim of recirculation. And the lowest victim is R3 as have the gain more mass flow rate absorption respect to R1. RTI value for all three racks are above the desired value but it's not too far from common data centers. **Fig 23** is showing the RTI value in different CRAH supply temperature. By different simulation, the average value of server and CRAH return temperature was changing and the reason of this fluctuation was not clear for me.

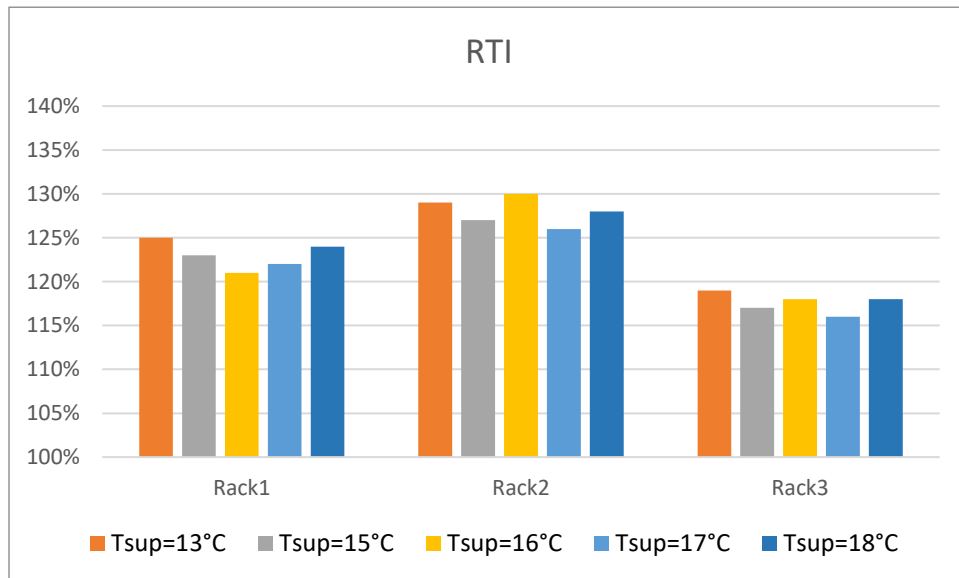


**Fig 23.** RTI (%) by  $T_{\text{Ref}}$   $13^{\circ}\text{C}$ ,  $15^{\circ}\text{C}$ ,  $16^{\circ}\text{C}$ ,  $17^{\circ}\text{C}$ ,  $18^{\circ}\text{C}$

### 3.5 Supply and return heat indices

Reminding, SHI Fig 24 and RHI Fig 25, are complimentary of each other are another thermal performance efficiency of the data center which is about the air flow energy efficiency[32]. as it was expected the supply temperature doesn't influence on these parameters but some unexpected fluctuating in different simulation report may influence the non-accuracy of these parameters, ideal value for SHI is 0 and RHI consequently 100%, while the standard value for these parameters are less than 20% SHI and more 100% for RHI, however, these values in common data center are reaching up to ~40% and 60%. R3 respect to other two racks have slightly better value.

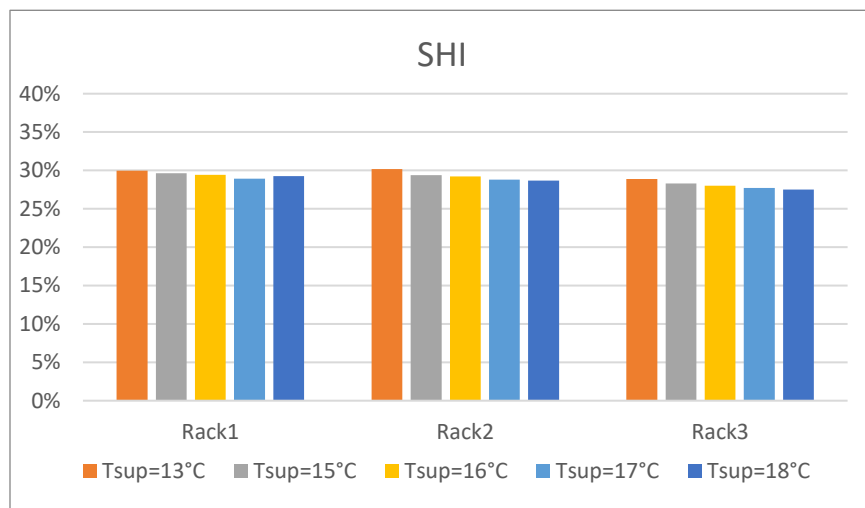


**Fig 24.** SHI (%) by  $T_{Ref}$  13°C,15, °C,16°C,17°C,18°C

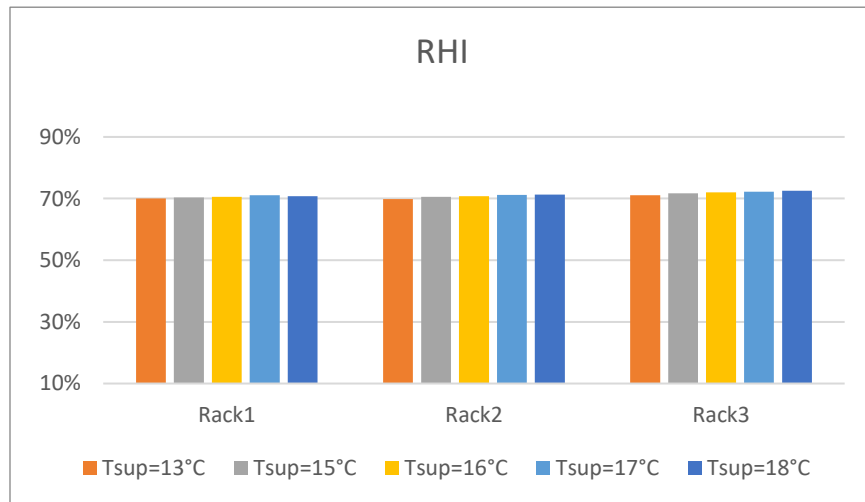


**Fig 25.** SHI (%) by  $T_{Ref}$  13°C,15, °C,16°C,17°C,18°C

## Chapter 4

### 4.1. Effect of adding partitions on thermal metrics

In the previous chapter I optimized the supply temperature of CRAH in DC/RL respecting the ASHRAE thermal user guide. Since the health of server rack has the most priority in data centers maximum supply temperature I proposed in CRAH was 16°C although  $RCI_{Lo}$  has the lower efficiency respect the supply temperature 17°C. In this chapter, I analyse the effect of different layout on thermal metrics respecting to the ASHRAE thermal guideline and by verifying the thermal metrics parameters, that proposed [32]. I proposed the supply CRAH temperature 17°C for all layout by intention to verify if any case has can let us increase the inlet temperature and we can satisfy the thermal efficacy standards. proposed layouts are based on the minimum cost of installation and modification in the current Data center. There were others such as changing the plenum height, changing the distance of rack room wall, changing the distance of tile from racks and other different configuration. I study 3 different layouts:

- Effect of adding cold aisle contaminate
- Effect of Closing a portion of under floor
- Effect of Closing the upper part of the racks

The idea of adding cold aisle contaminate and closing the upper part of the rack is to understand the influence of partition on cold and hot flow, both partition separate close the upper part of the rack and avoid the air recirculation coming from the top of the rack. it is expecting in both scenarios observing diminution Level of air recirculating and the percentage of reeducation is important to realize the airflow path. And the idea of closing a portion of underflow plenum is that if reducing the volume of the plenum and consequently increase of velocity has an effect on thermal metrics. Note that in all three scenarios the mass flow rate of servers considered constant, but it may be influenced by the by changing the configuration of the data center. And since there is we don't have information about the effect of server mass flow rate intake by modification of the configuration of the data center, I choose the scenarios that may have the least effect on variation of server mass flowrate.

### 4.1.1. Roof containment

As **Fig. 36** by adding roof contaminate on top of the racks along the wall the effect of air recirculation coming from top of the racks are reduced and as it is showing in **table 18** Alike the normal layout the coldest server is the bottom sever of middle rack but the hottest server unlike the other scenarios the instead of the top server of R1, the hottest server is R3 and the temperature of bottom servers except the middle rack increased slightly, and as it is showing in the **Fig.32** the two cold regions in front of the racks are faded, and the velocity vectors are less circular, in counterclockwise direction, the reason is that a portion of cold air by arriving at top of the roof change their direction and in contour clockwise and turn around the server racks this air could influence the R1 and reduce its temperature that was in normal layout was the hottest server rack.in addition, as it is showing in the other two cold spots located near CRAHs are nearly are faded because the air has more kinetic energy. The presence of roof contaminant causes a better air distribution in the room. none of the inlet server rack average temperature exceeds to 27°C that means all server racks are in health from over temperature point of view. The  $RCI_{Hi}$  value for all three racks is 100% as showing in **Fig.32** Consequently, it can say that presence of roof contaminant has a positive effect on  $RCI_{Hi}$  **Fig 26** thermal evaluation which hast the most priority in the data center. as it is showing in **table 18**, As it is adding roof contaminate increase the average temperature of first and second-row server racks while reducing the third and fourth row, these increase temperatures are more tangible at sided racks (R1, R3).  $RCI_{Io}$  **Fig.27** value increased in R1 and R2 which doesn't expect and in R3 does not influence as it is showing in photo **Fig. 32** the value of RTI **Fig.28** decreases ~8% in this layout the CRAH return temperature remain nearly the same respect to normal layout while the  $\Delta t$  equipment increase which is positive news. SHI and RHI values in R1 and R2 demonstrate a better value respect a normal configuration **Fig 29,30**.

Rack N	Supply	Return	Supply	Return	Supply	Return	Supply	Return
R1	17.52	27.03	17.73	27.50	19.19	28.98	25.15	34.05
R2	17	26.16	17.24	26.55	18.44	27.55	23.37	31.57
R3	17.73	27.61	18.34	28.38	21.26	30.84	26.61	35.34

**Table 18.** Average supply and return temperature servers by  $T_{Ref}$  17°C with roof containment layout(from bottom to top in horizontal line)

#### 4.1.2. Partial closing of the plenum

In this layout, a vertical partition along the X-axis applied to reduce 30% of the underfloor plenum volume( near R3). Alike normal layout the coldest server is the bottom server of the middle rack and the hottest one is the top server of the first rack. **Table 19** is showing that the inlet temperature of all three racks increases respect a normal layout this temperature augmentation is less evident in the middle chassis. The temperature of all the 4<sup>th</sup> row of chassis is increased and R1 and R2 are exceeding the maximum recommended temperature so the  $RCI_{Hi}$  **Fig.26** value decreased in R1 and R2 and only R3 doesn't a victim of the decrement. The result of, the result of temperature increment in the first and second row of the racks causes the  $RCI_{Lo}$  **Fig.27**value slightly increased respect to normal layout.  $RTI$  **Fig.28** value increased in all three racks especially in the first rack, and the major reason is that the temperature difference in the equipment is decreasing while the CRAH temperature is nearly remained constant, respect to normal layout.  $SHI$  and  $RHI$  **Fig.29,30** respect to normal layout remain are slightly increasing as it is and the reason is that the temperature difference of equipment in this layout respect to normal layout has a smaller value and this is not a good thing, however decreasing the  $RHI$  and increasing  $SHI$  are not notable, but it can say except  $RCI_{Lo}$  all the thermal matrices are decreased and it means partial closing of plenum has a negative effect on efficiency of data center. **Fig.34,38** do not show the major difference with normal layout **Fig. 31,35**.

Rack N	Supply	Return	Supply	Return	Supply	Return	Supply	Return
R1	17.48	26.6	17.71	27.15	19.63	29.2	28.31	36.78
R2	17.02	26.17	17.3	26.7	20.15	29.1	28.02	35.92
R3	17.97	27.65	18.6	28.4	20	29.81	26.39	35.43

**Table 19.** Average supply and return temperature servers by  $T_{Ref} 17^{\circ}C$  with partial closing plenum layout(from bottom to top in horizontal line)

### 4.1.3. Vertical partition on top of the racks

As it is showing in **Fig. 37** in this layout a vertical partition from top of the racks to the ceiling applied to close the upper part of the racks. **Table 20** showing that like the other scenarios the coldest server is the bottom server of the middle rack with the same temperature equal to the CRAH supply temperature and the hottest one is the top server of the first rack. the supply temperature of first and second rows of chassis are unlike the roof containment layout, also respect the normal layout the intake server temperature is decreasing in the first and second row of chassis, in the third and fourth chassis the intake server temperature are increasing **Fig. 33** respect to both normal and roof containment layout. For example, in the normal layout, roof containment and in the current layout the bottom server of R1 temperatures are  $17.41^{\circ}C$ ,  $17.48^{\circ}C$  and  $17.37^{\circ}C$  while this value for the top server of the equal rack are  $28.27^{\circ}C$ ,  $25.15^{\circ}C$  and  $29.57^{\circ}C$  which shows that this scenario has a negative effect in both RCI thermal metrics ( $RCI_{Hi}$  and  $RCI_{Lo}$ ). Reminding that desirable temperature value for rack inlet according to ASHRAE is between  $18^{\circ}C - 27^{\circ}C$ . The presence of a vertical partition on top unexpectedly increases the temperature of three top servers. The value for  $RCI_{Hi}$  as it is showing in **Fig 26** decreased to 4% in R1 and 1% but although the temperature of the top server of R1 increased but doesn't hit the recommended temperature. This layout shows that the air-recirculation from the side of the racks influenced more respect to normal

layout. The value as it is showing in **Fig 27** for  $RCI_{Lo}$  is also decreased respect to the normal layout that means that the air- recirculation doesn't because of the lower density couldn't reach the lower part of the racks and cold air flow was dominant in lower servers.  $RTI$  **Fig 28**.value decreased specially in sided racks (R1, R2), return CRAH temperature remained nearly constant while the average temperature of inlet and outlet racks R1, and R2 respect to normal layout increased.  $SHI$  and  $RHI$  **Fig 29,30** value respect to normal layout except to normal layout slightly increasing and decreasing

Rack N	Supply	Return	Supply	Return	Supply	Return	Supply	Return
R1	17.37	26.87	17.54	27.39	20.56	30.35	29.57	38.22
R2	17	26.14	17.21	26.61	20.32	29.29	28.16	35.96
R3	17.67	27.54	17.89	27.99	20.14	30.05	26.87	35.81

**Table 20.** Average supply and return temperature servers by  $T_{Ref}$  17°C with vertical partition layout(from bottom to top in horizontal line)

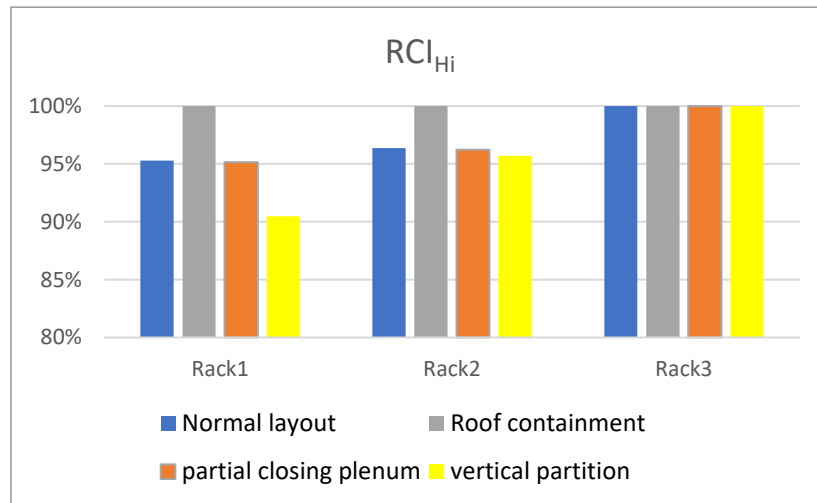


**Fig 26.** Effect of different layout on  $RCI_{Hi}$  (%)

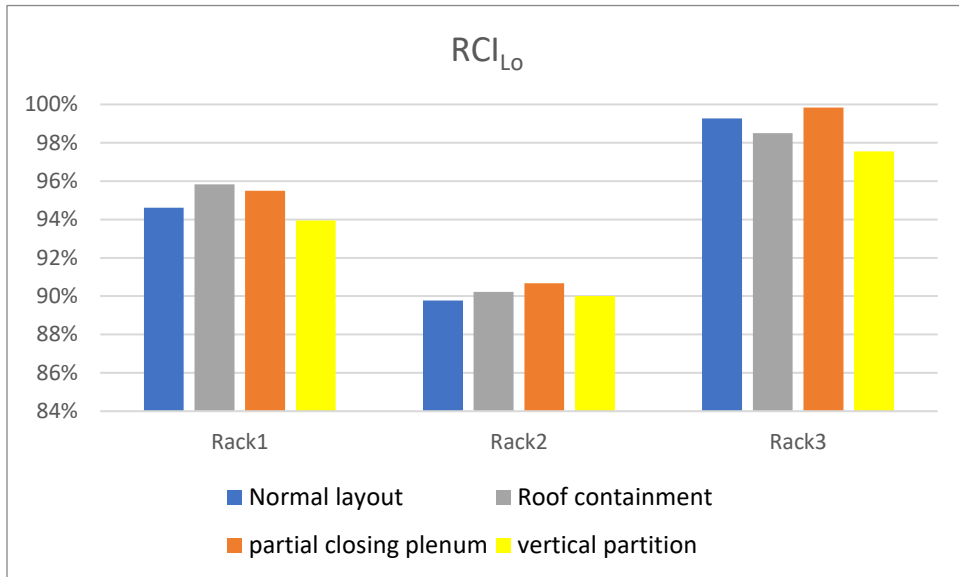


**Fig 27.** Effect of different layout on RCI<sub>Lo</sub> (%)

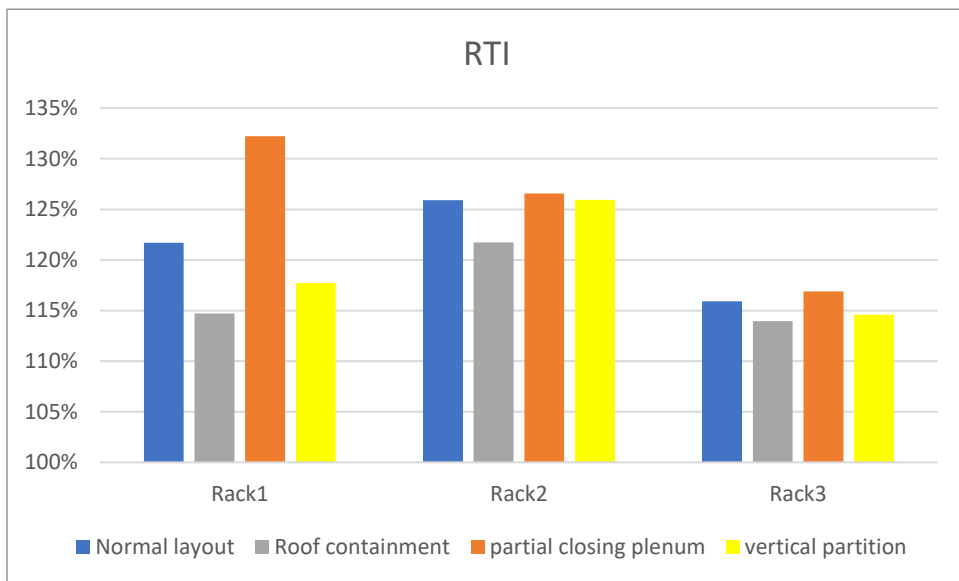


**Fig 28.** Effect of different layout on RTI (%)

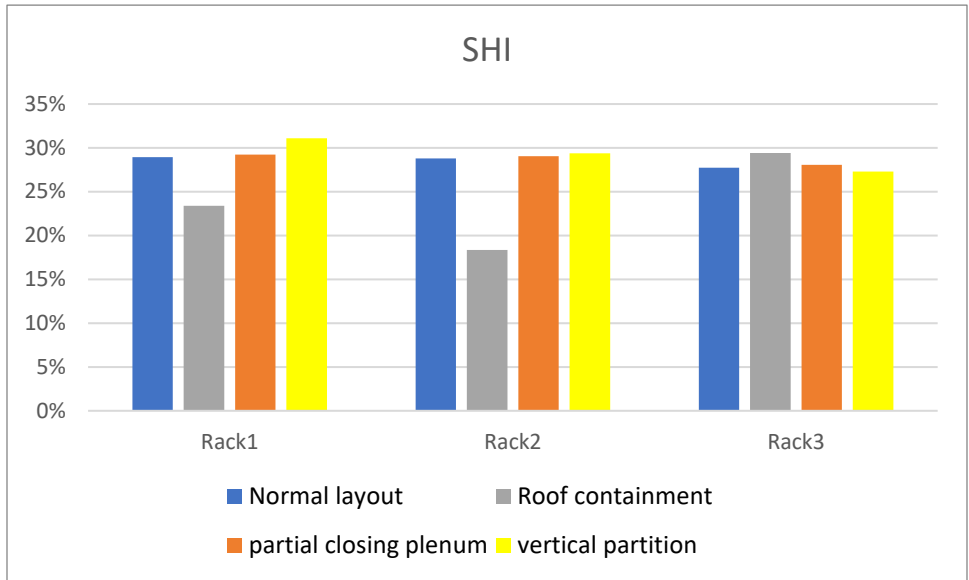


**Fig 29.** Effect of different layout on SHI (%)

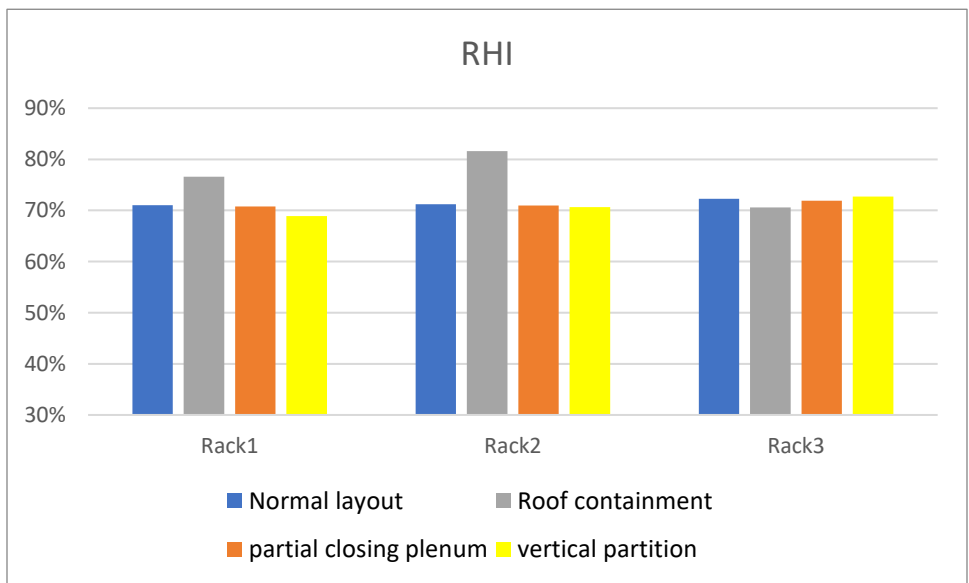


**Fig 30.** Effect of different layout on SHI (%)

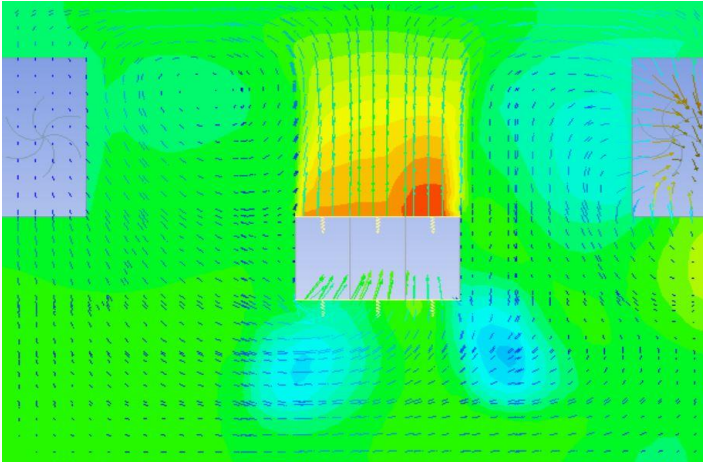


**Fig. 31** Normal Layout

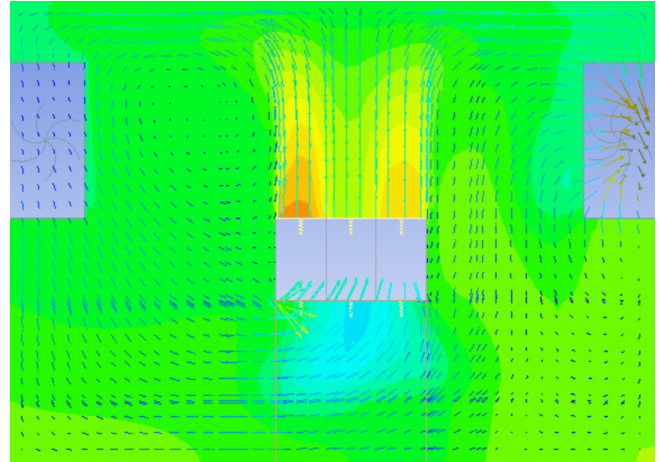


**Fig. 32** Roof containment layout

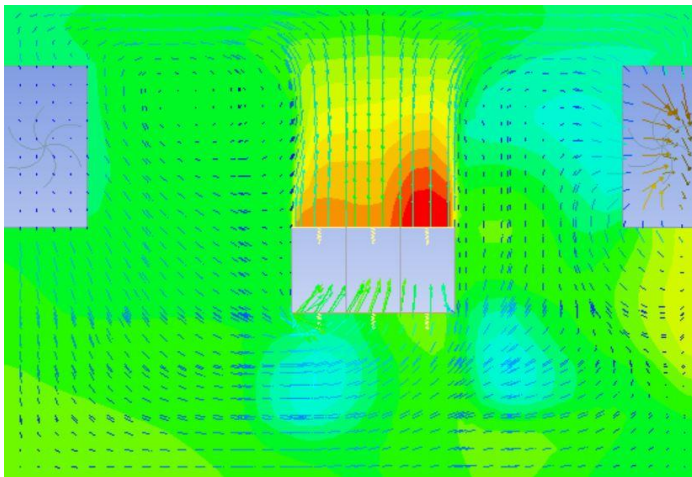


**Fig. 33** Vertical partition on the rack

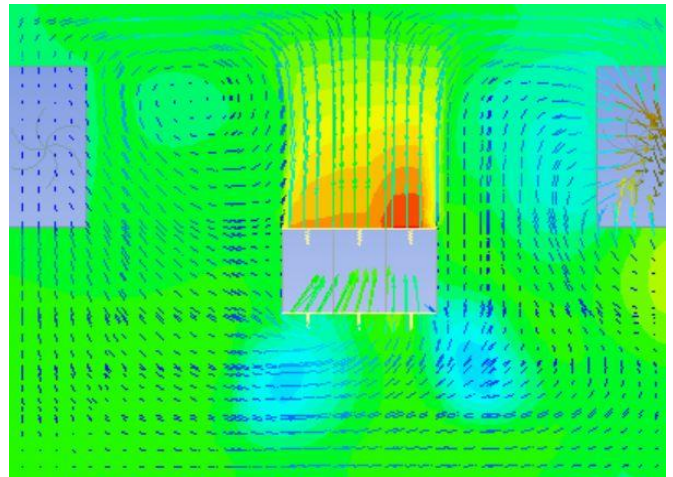


**Fig. 34** Partial closing plenum

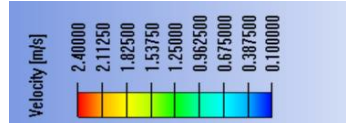
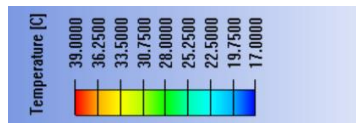


**Fig. 31,32,33,34** The temperature contours and velocity vector in XZ plane

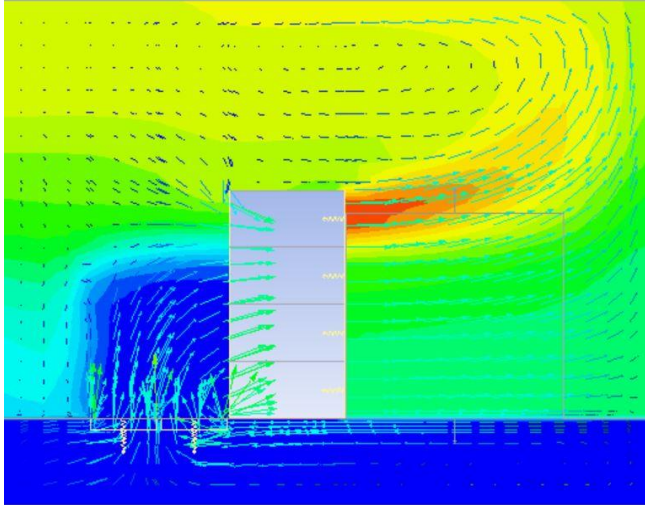


**Fig. 35** Normal Layout

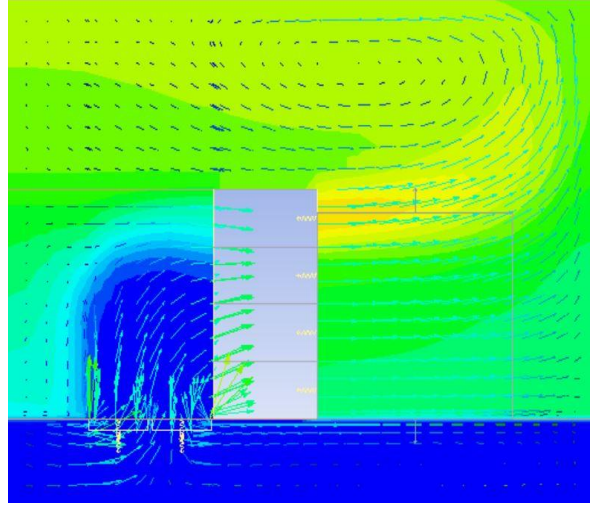


**Fig. 36** Roof containment layout

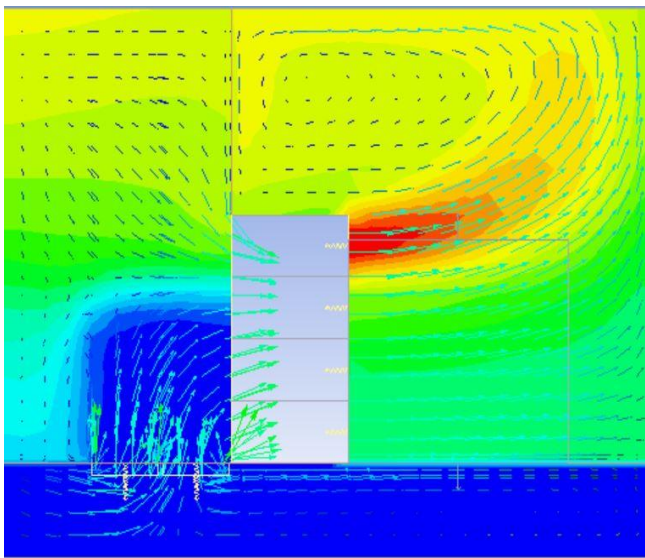


**Fig. 37** Vertical partition on the rack

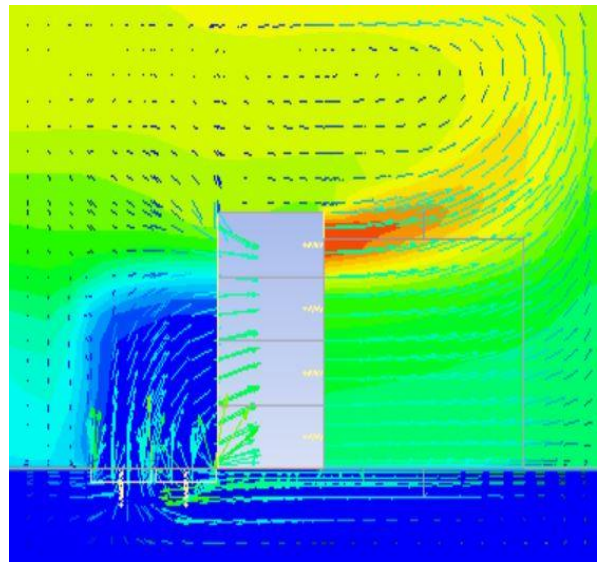


**Fig. 38** Partial closing plenum

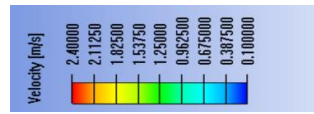
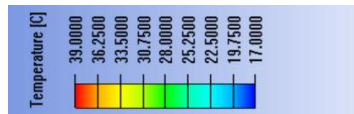


**Fig. 35,36,37,38** The temperature contours and velocity vector in YZ plane at the middle of R1

## 4.2. Effect of rack power density on thermal metrics

In current study, I analyses the effect of increasing power density of the racks on thermal metrics, in DC/RL the power of each rack in the steady-state study considered 15kW, in the current study, I increased the power the rack power in 16.5kW, 18kW, 21kW and calculate the thermal metrics. As it is showing in **table 21, 22, 23, 24** the inlet temperature of all server racks increment is more sensible in the fourth row of server racks. The supply temperature of the lowest level of R1 and R2 nearly remained constant by increasing the power density and only the R3 is influenced slightly by increasing power density, the return temperature of all lowest level of server racks are increasing by increasing power density the lowest temperatures are in middle servers. For example, the temperature difference in the middle racks is increasing from 9.07°C, 9.97°C, 10.88°C and 12.70°C for normal rack power, 10%, 20%, 40% of rack power. While this temperature increment in the top middle server rack is 8.05°C, 8.83°C, 9.57°C, and 11.17°C. that means the increasing power density on the lower server is much more than the upper servers. In all scenario top server of R1 which the closest rack to CRAH1 the hottest temperature and this temperature have increased from 35.54°C, 38.02°C, 40.11°C and 44.50°C. and the first middle server racks has the lowest temperature and increase of power does not affect on intake temperature and it reminds constantly in all scenario (16°C). **Fig 44, 45, 46, 47** shows that by increasing power density not only the temperature but also the velocity in the back of the racks are increasing, the increment of velocity is more evident on the right upper part of the room by increasing the power density, **Fig. 47** is also showing that the direction of velocity vectors the flow the recirculating airflow coming from the upper part of the rack and reentering the intake servers, the velocity value is  $\sim 0.3 \text{ m/s}$  at the middle distance of top of the racks and roof, the velocity has the minimum value near to the wall region and just on top of the racks, it is also can observed by designing the under floor region and not imposing the mass flow rate of tiles in boundary condition, showing that the velocity profile at the exit of tile is not uniform. The velocity at the exit of the racks are horizontal and uniform and have the maximum value in this zone. the velocity of rack rear server thanks to four fans provide a high kinetic energy that by arriving to the wall the velocity is still has a high value and is the only surface that the velocity is not near minimum value.

**Fig. 39** is showing that the  $RCI_{Hi}$  is decreasing as the inlet temperature increasing like other scenarios only the top server racks are victim of this value and for the normal power density none of the three racks are not reaching the maximum recommended value according to ASHRAE by increasing 10% pf power the top middle server exceeding the recommended value, that shows that the middle rack is more sensible respect to other sided servers, by increasing the power to 20% respect to normal power all three racks infract the recommended limit temperature and by increasing the power density up to 40% , all the three servers are with more difference out of the recommended value and the top server of middle rack not only hit the maximum recommended value but also hit the maximum allowable temperature (32°C) [12], vice versa the value of  $RCI_{Lo}$ .

**Fig. 40** increasing alike other scenarios the first and second rows of servers are usually victims of this limitation, the intake temperature of the bottom servers are the least influenced by increasing power density as it is showing on the **tables 21,22,23,24**, as it is mentioned before the average intake temperature of the three out of four servers of middle rack remained constant respect to default power, by increasing 40% of power. In the third row of the server only R1 reach the minimum recommended temperature and the other racks were still under the remanded limitation. As it is showing **Fig. 41**, RTI value is increasing as the power density is enhancing in the default power and the reason is that the temperature difference of supply and return of CRAH is increasing more than the average temperature amputation of each rack by enhancing the power density, especially in R2, for example by increasing 40% of rack power density, this value increase from 130% arrived at 142% in middle rack. in all scenario the middle rack has the most recirculation value that means the temperature augmentation in the equipment respect to R1 and R3 is less and the reason is that thanks to cold airflow of side tiles the temperature intake of R1 and R3 is slightly lower than R2 so the temperature difference of upper side server is higher so RTI value has a lower value .SHI and RHI as it is showing in Fig.42,43 value are increasing and decreasing slightly by increasing power density the reason is that both average temperature of inlet and outlet of the racks are increasing but outlet temperature is increasing more, according to the equitation of SHI, the denominator value increasing more respect to the numerator. Also, the **Fig.44,45,46,47** demonstrating that increasing the rack power temperature at the front and back of the rack are increasing while temperature increment at the back of the is much more evident. Presence of recirculation starting from top back of the rack due to the high-density variation and influence more on the top inlet of server racks.

Rack N	supply	return	supply	return	supply	return	supply	return
R1	16.35	25.93	16.38	26.15	17.09	27.18	26.25	35.54
R2	16	25.07	16.11	25.35	17.70	26.64	26.48	34.53
R3	16.87	26.85	16.85	27.03	17.92	28	25.34	34.78

**Table 21.** Average supply and return temperature servers by  $T_{Ref}$  16°C with P=15kW layout(from bottom to top in horizontal line)

Rack N	supply	return	supply	return	supply	return	supply	return
R1	16.36	26.9	16.39	27.13	17.18	28.3	27.86	38.02
R2	16	25.97	16.11	26.27	17.93	27.76	28.01	36.84
R3	16.87	27.84	16.85	28.05	18.15	29.21	26.51	36.88

**Table 22.** Average supply and return temperature servers by  $T_{Ref}$  16°C with P=16.5kW layout(from bottom to top in horizontal line)

Rack N	supply	return	supply	return	supply	return	supply	return
R1	16.36	27.85	16.4	28.12	17.42	29.44	29.11	40.11
R2	16	26.88	16.11	27.19	18.19	28.83	29.49	39.06
R3	17	28.98	17.02	29.25	18.87	30.72	28.01	37.55

**Table 23.** Average supply and return temperature servers by  $T_{Ref}$  16°C with P=18kW layout(from bottom to top in horizontal line)

Rack N	supply	return	supply	return	supply	return	supply	return
R1	16.41	29.83	16.46	30.14	17.51	31.60	31.68	44.50
R2	16	28.70	16.12	29.05	18.66	31.08	32.97	44.14
R3	17.07	31.03	17.10	31.40	19.88	33.77	30.84	43.94

**Table 24.** Average supply and return temperature servers by  $T_{Ref}$  16°C with P=15kW layout(from bottom to top in horizontal line)

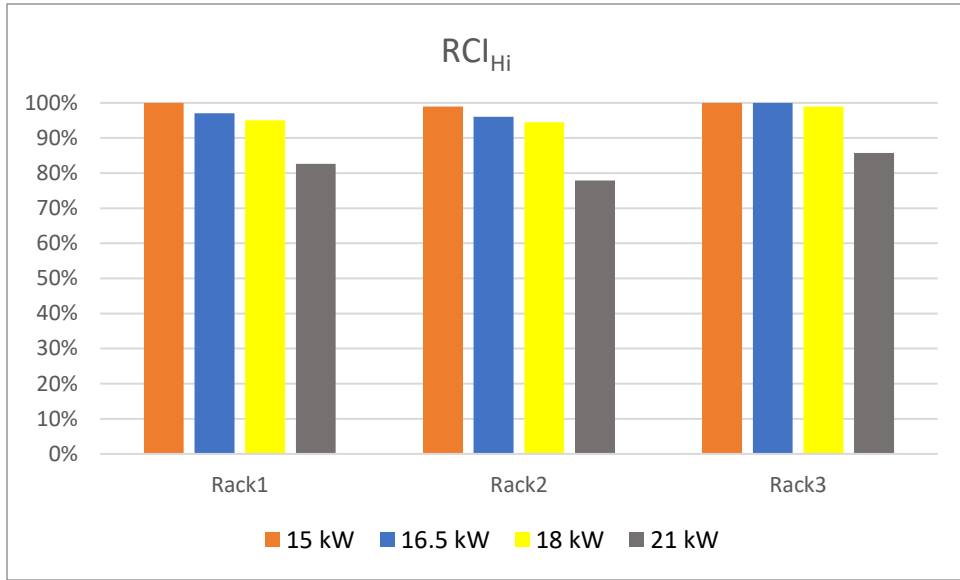


**Fig. 39** Effect of increase of power on RCI<sub>Hi</sub> (%)

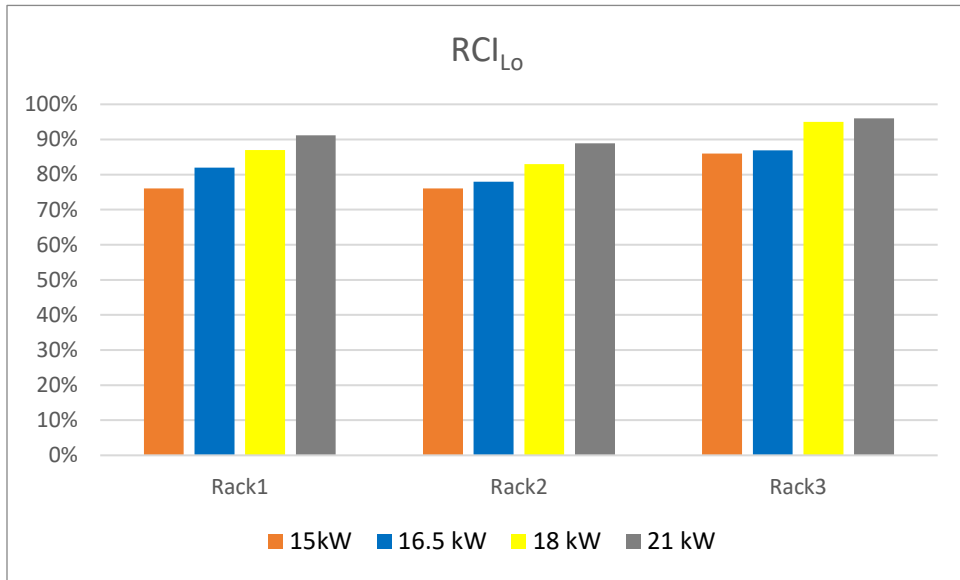


**Fig. 40** Effect of increase of power on RCI<sub>Lo</sub> (%)

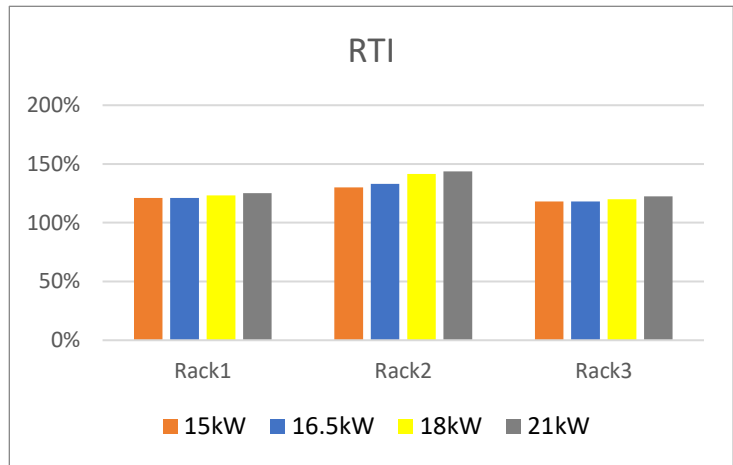


**Fig. 41** Effect of increase of power on RTI (%)

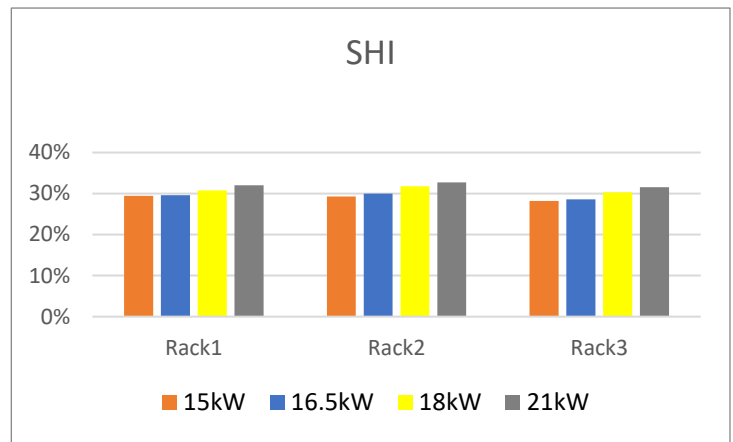


**Fig. 42** Effect of increase of power on SHI (%)

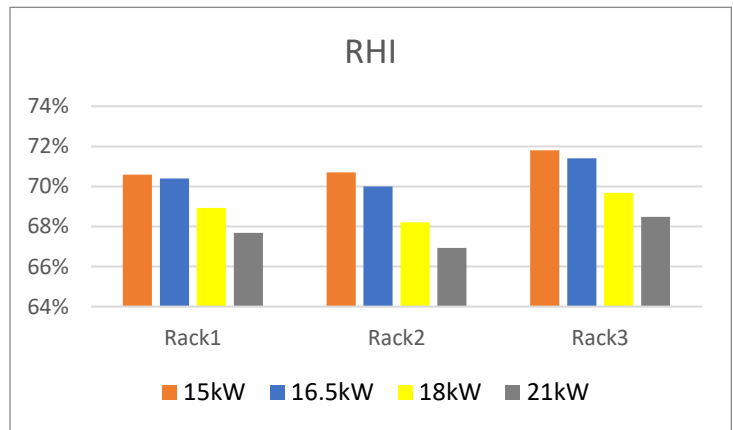


**Fig. 43** Effect of increase of power on RHI (%)

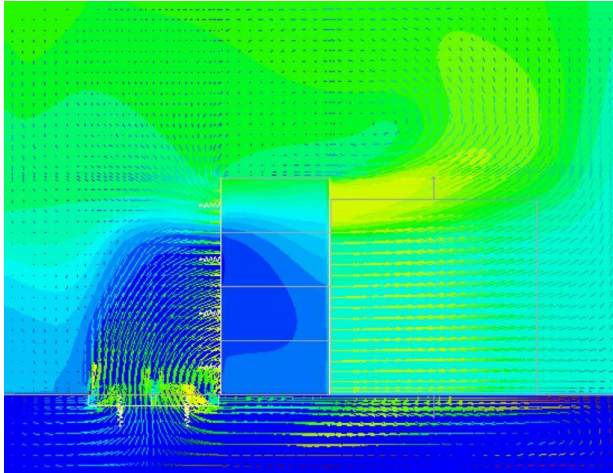


Fig. 44 P=15kW

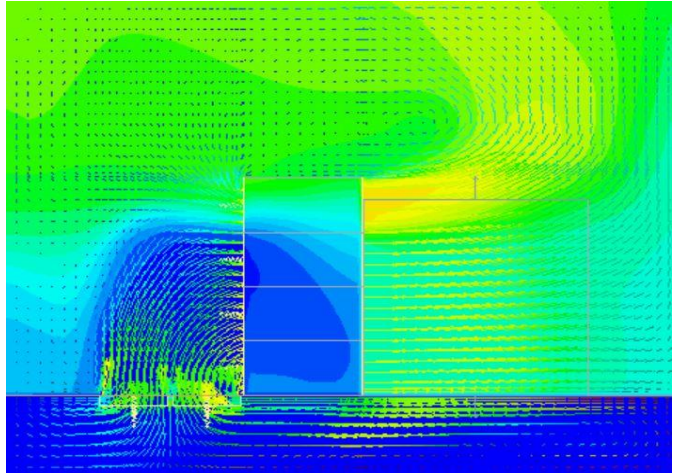


Fig. 45 P=16.5kW

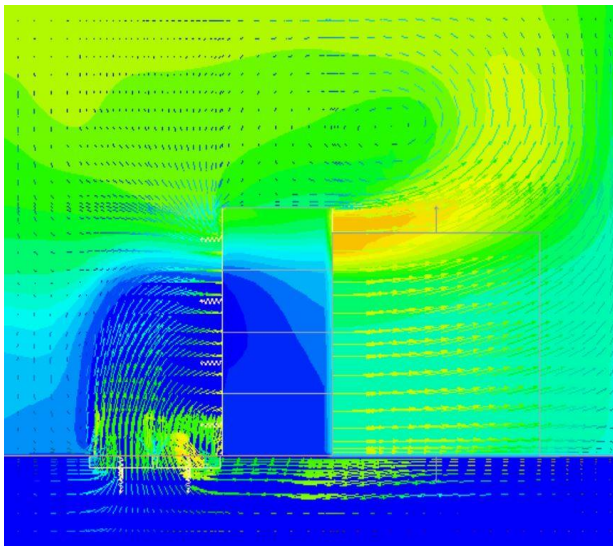


Fig. 46 P=18kW

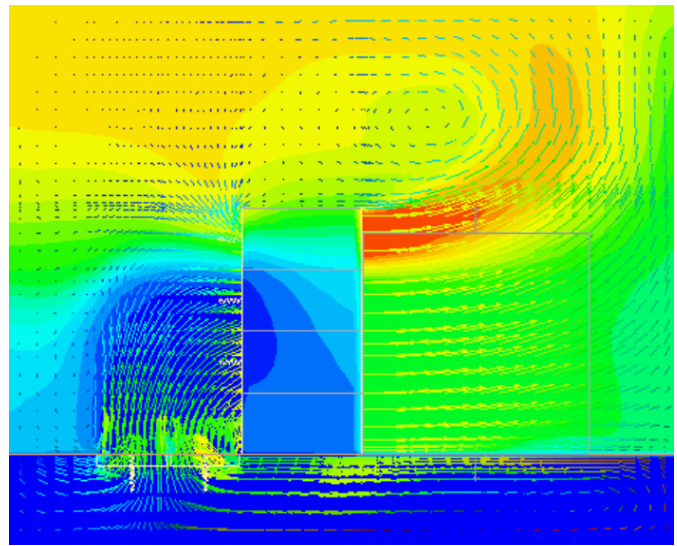


Fig. 47 P=21kW

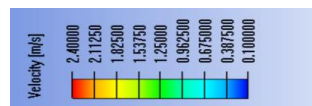
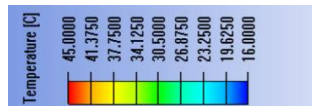


Fig. 44,45,46,47 The temperature contours and velocity vector in YZ plane at the middle of R1

## Conclusion :

The goal of this work was simulating a real data center and validate it against the experimental data, which is working nearly in standard condition. However, the configuration of recent data center is different, results showed that the girding size doesn't make a significant difference in temperature distribution in data center, the result shows that Realizable k-epsilon turbulence model has more accurate result in separating plane and the round jets respect to normal k-epsilon turbulence model, since in back of the racks and exit of the perforated tiles this phenomenon is happening, and consequently a better result in general temperature distribution in data center is observed. In all simulation with normal configuration of the model is observed that the Rack nearest to the CRAH (especially the top server) not only has the warmest intake and exit temperature, but also the has the maximum temperature difference respect to other racks. And the middle rack has the lowest temperature intake and exit of the rack since digesting the greatest portion of mass flow rate respect to other two racks. Unfortunately, the information of temperature at the inlet and outlet of the server rack was not presented in the experimental test, to compare the thermal metrics efficiencies with experimental data, so considered the average temperature of each server rack and tiles for parametric calculating of five thermal matrices  $RCI_{Hi}$ ,  $RCI_{Lo}$ , RTI, SHI and RHI. The results show the  $RCI_{Lo}$  value was significantly lower than the recommended value by ASHRAE for the current type of data center. By selecting different supply temperature of CRAC I understand we can increase the CRAC supply temperature up to 16°C and we can guarantee the reliability of the server according to ASHRAE maximum recommendation temperature for intake of server [12]. In all simulation, the average temperature of server, CRAH inlet and has considered. Note that in report shows different average temperature, that influenced on the charts especially RTI chart. In all simulation, it is observed the middle rack has the highest value of RTI and the rack with the highest distance from the CRAH has the minimum value of RTI. Different partition has applied to understand the effect of them on thermal metrics. Vertical and horizontal partitions were used to reducing the recirculating the result shows that horizontal partition (roof containment) plays a very important role in reducing  $RCI_{Hi}$ , RTI, and SHI (R2 and R3) value respect to normal layout, while vertical presence of partition has a negative effect in  $RCI_{Hi}$  and decreased the value of RTI only in the sided racks. While doesn't influence on SHI

value respect to normal layout. The only significant issue of the presence of vertical plenum under the raised floor (near the R3) was increasing the RTI value in the R1. By increasing the power  $RCI_{Hi}$  increased and  $RCI_{Lo}$  decreased while the RTI increased and the SHI value decreased proportionally.

In this work, I tried another study such as the effect of sided tiles and full enclosure, but the result shows strange values and I figured out the changing the configuration of data center highly depend on the mass flow rate of the racks, that need to measure and impose in boundary condition of the server.

## References:

- [1] X. Jim, F. Zhang, A. V. Vasilakos, Z. Liu, Green data centers: a survey, perspectives, and future directions, arXiv Prepr. (2016), asXiv 1608.00687.
- [2] P.X. Gao, A.R. Curits, W. Bernard, S. Keshav, It's not easy being green, ACM SIGCOMM Compute. Commun. Rev.42 (4) (2011) 211-222.
- [3] Baptiste Durand-Estebe, Cédric Le Bot, Jean Nicolas Mancos, Eric Arquis, Data center optimization using PID regulation in CFD simulations, Energy and Buildings 66 (2013) 154–164
- [4] M. Salim, R. Tozer, Data Centers' energy auditing and benchmarking-progress update, ASHRAE Trans. 116 (2010) 1.
- [5] Z. Song, Numerical cooling performance evaluation of fan-assisted perforations in a raised-floor data center, International Journal of Heat and Mass Transfer 95 (2016) 833–842
- [6] J. Cho, T. Lim, B.S. Kim, Measurements and predictions of the air distribution systems in high compute density (Internet) data centers, Energy Build. 41 (10) (2009) 1107–1115.
- [7] ASHRAE Technical Committee 9.9, Mission Critical Facilities, Technology Spaces, and Electronic Equipment, Thermal Guidelines for Data Processing Environments, American Society of Heating, Refrigerating and Air-Conditioning Engineers Inc., 2008.
- [8] E. Wibron, A. L. Ljung, T. S. Lundström, Computational Fluid Dynamics Modeling and Validating Experiments of Airflow in a Data Center [www.mdpi.com/journal/energies](http://www.mdpi.com/journal/energies) Energies 2018, 11, 644; doi:10.3390/en11030644.
- [9] <http://www.afs.enea.it/project/neptunius/docs/fluent/html/th/node11.htm>
- [10] J. Choa, B. Sean Kimb, Evaluation of air management system's thermal performance for superior cooling efficiency in high-density data centers Energy and Buildings 43 (2011) 2145–2155.
- [11] B. Watson, V. Kumar Venkiteswaran, Universal Cooling of Data Centres: A CFD Analysis, 9<sup>th</sup> International Conference on Applied Energy, ICAE2017, 21-24 August 2017, Cardiff, UK.
- [12] ASHRAE TC9.9, Thermal Guidelines for Data Processing Environments, Fourth Edition, ASHRAE, Atlanta Georgia, 2015.
- [13] R.K. Sharma, C.E. Bash, C.D. Patel, Dimensionless parameters for evaluation of thermal design and performance of large-scale data centers, in: Proceedings of AIAA2002-3091.
- [14] M.K. Herrlin, Airflow and cooling performance of data centers: two performance metrics, ASHRAE Transactions 114 (2) (2008).

- [15] M.K. Herrlin, Improved data center energy efficiency and thermal performance by advanced airflow analysis, in: Proceedings of Digital Power Forum, 2007, pp.10 –12.
- [16] M.K. Herrlin, Rack cooling effectiveness in data centers and telecom central offices: the rack cooling index (RCI), ASHRAE Transactions 111 (2) (2005) 1–11.
- [17] Emerson Network Power, Energy logic: Reducing Data Center Energy Consumption by Creating Savings that Cascade Across Systems, A White Paper from the Experts in Business Critical Continuity, 2008.
- [18] bdelmaksoud, W., Khalifa, H. E., Dang, T. Q., Schmidt, R., and Iyengar, M.,2010 , “Improved CFD Modeling of a Small Data Center Test Cell,” Proceedings of the Intersociety Conference on Thermal Phenomena in Electronic Systems (ITherm), Las Vegas, June 2–5.
- [19] Tate Inc., 2013, “Tate Access Floors,” [www.tateinc.com](http://www.tateinc.com).
- [20] Waleed A. Abdelmaksoud, Thong Q. Dang, H. Ezzat Khalifa, Roger R. Schmidt, Improved Computational Fluid Dynamics Model for Open-Aisle Air-Cooled Data Center Simulations, Journal of Electronic Packaging, SEPTEMBER 2013, Vol. 135 .
- [21] <https://www.sharenet.ca/Software/Fluent6/html/ug/node480.htm>
- [22] Abdelmaksoud, W., 2012, “Experimental and Numerical Investigations of the Thermal Environment in Air-Cooled Data Centers,” Ph.D. thesis, Department of Mechanical and Aerospace Engineering, Syracuse University, Syracuse, NY.
- [23] H.S. Erden, M. Koz, M.T. Yildirim, H.E. Khalifa, Experimental demonstration and flow network model verification of induced CRAH bypass for cooling optimization of enclosed-aisle data centers, IEEE Trans. Compon., Packag. Manuf. Technol. 7 (11) (2017) 1795–1803.
- [24] V. Kumar, S. Kapoor, G. Arora, S. Saha, P. Dutta, A combined CFD and flow network modelling approach for vehicle underhood air flow and thermal analysis, SAE Int. (2009) 1–7.
- [25] J. Rambo, Y. Joshi, Modeling of data center airflow and heat transfer: state of the art and future trends, Distrib. Parallel Databases 21 (2007) 193–225.
- [26] [https://www.sharcnet.ca/Software/Ansys/16.2.3/enus/help/ice\\_ug/ice\\_ug\\_sec\\_macro\\_rack.html](https://www.sharcnet.ca/Software/Ansys/16.2.3/enus/help/ice_ug/ice_ug_sec_macro_rack.html)
- [27] H. Fernando, J. Siriwardana, S. Halgamuge, Can a data center heat-flow model be scaled down? Information and Automation for Sustainability (ICIAfS), in: Proceedings of IEEE 6th International Conference on Information and Automation for Sustainability, 2012.
- [28] Waleed A. Abdelmaksoud, Thong Q. Dang, H. Ezzat Khalifa, Roger R. Schmidt, Perforated Tile Models for Improving Data Center CFD Simulation, 13<sup>th</sup> IEEE IThERM Conference (2012)IEEE.

[29] [https://www.sharcnet.ca/Software/Ansys/16.2.3/enus/help/ice Ug/ice Ug\\_sec\\_macro\\_crac.htm](https://www.sharcnet.ca/Software/Ansys/16.2.3/enus/help/ice Ug/ice Ug_sec_macro_crac.htm)

[30] <https://www.sharcnet.ca/Software/Fluent6/html/ug/node482.htm>

[31] [https://www.sharcnet.ca/Software/Ansys/16.2.3/enus/help/ice Ug/ice Ug\\_sec\\_start\\_gen\\_mesh.html](https://www.sharcnet.ca/Software/Ansys/16.2.3/enus/help/ice Ug/ice Ug_sec_start_gen_mesh.html)

[32] A. Capozzoli, G. Seralea, L. Liuzzoa, Marta Chinnicib, Thermal metrics for data centers: a critical review 6th International Conference on Sustainability in Energy and Buildings, SEB-14

[33] Deep V. Sheth, Sandip K. Saha\* Numerical study of thermal management of data centre using porous medium approach Journal of Building Engineering 22 (2019) 200–215

[34] Emerson Network Power, Energy logic: reducing data center energy consumption by creating savings that cascade across systems. A White Paper from the Experts in Business-Critical Continuity; 2008.

[35] Cho, J. Yang, W. Park, Evaluation of air distribution system's air flow performance for cooling energy savings in high-density data centers, Energy Build. 68(2014)270–279.

Dry bulb Temperature [°C]	Humidity Range [%]	Maximum dew point [°C]	Maximum Rate of change [°C/h]
18 to 27	5°C DP to 60 % and 1°C DP		
15-32	20-80	17	5/20
10-35	20-80	21	5/20
5-40	-12°C DP & 8-80	24	5/20
5-45	8-80	24	